Subscriber access provided by UNIV OF CAMBRIDGE

Article

Amphiphilic Diblock Terpolymer PMAgala-b-P(MAA-co-MAChol)s With Attached Galactose and Cholesterol Grafts and Their Intracellular pH-responsive Doxorubicin Delivery

Zhao Wang, Ting Luo, Ruilong Sheng, Hui Li, Jingjing Sun, and Amin Cao

Biomacromolecules, **Just Accepted Manuscript** • DOI: 10.1021/acs.biomac.5b01227 • Publication Date (Web): 18 Dec 2015

Downloaded from http://pubs.acs.org on December 25, 2015

Just Accepted

"Just Accepted" manuscripts have been peer-reviewed and accepted for publication. They are posted online prior to technical editing, formatting for publication and author proofing. The American Chemical Society provides "Just Accepted" as a free service to the research community to expedite the dissemination of scientific material as soon as possible after acceptance. "Just Accepted" manuscripts appear in full in PDF format accompanied by an HTML abstract. "Just Accepted" manuscripts have been fully peer reviewed, but should not be considered the official version of record. They are accessible to all readers and citable by the Digital Object Identifier (DOI®). "Just Accepted" is an optional service offered to authors. Therefore, the "Just Accepted" Web site may not include all articles that will be published in the journal. After a manuscript is technically edited and formatted, it will be removed from the "Just Accepted" Web site and published as an ASAP article. Note that technical editing may introduce minor changes to the manuscript text and/or graphics which could affect content, and all legal disclaimers and ethical guidelines that apply to the journal pertain. ACS cannot be held responsible for errors or consequences arising from the use of information contained in these "Just Accepted" manuscripts.

ACS Publications

Biomacromolecules is published by the American Chemical Society. 1155 Sixteenth Street N.W., Washington, DC 20036

Published by American Chemical Society. Copyright © American Chemical Society. However, no copyright claim is made to original U.S. Government works, or works produced by employees of any Commonwealth realm Crown government in the course of their duties.

Amphiphilic Diblock Terpolymer PMAgala-*b*-P(MAA-*co*-MAChol)s With Attached Galactose and Cholesterol Grafts and Their Intracellular pH-responsive Doxorubicin Delivery

*Zhao Wang, Ting Luo, Ruilong Sheng, Hui Li, Jingjing Sun and Amin Cao**

CAS Key Laboratory of Synthetic and Self-assembly Chemistry for Organic Functional Molecules, Shanghai Institute of Organic Chemistry, Chinese Academy of Sciences, 345 Lingling Road, Shanghai 200032, China

**Author for correspondence:*

Phone: +86-21-5492-5303, fax: +86-21-5492-5537

E-mail: acao@ sioc.ac.cn

ABSTRACT

In this work, a series of diblock terpolymer poly(6-*O*-methacryloyl-D-galactopyranose)-*b*-poly(methacrylic acid-*co*-6-cholesteryloxy hexylmethacrylate) amphiphiles bearing attached galactose and cholesterol grafts denoted as the PMAgala-*b*-P(MAA-*co*-MAChol)s were designed and prepared, and these terpolymer amphiphiles were further exploited as a platform for intracellular doxorubicin (DOX) delivery. First, employing a sequential RAFT strategy with preliminarily synthesized poly(6-*O*-methacryloyl-1,2:3,4-di-*O*-isopropylidene-D-galactopyranose) (PMAIpGP) macro-RAFT initiator and a successive TFA-mediated deprotection, a series of amphiphilic diblock terpolymer PMAgala-*b*-P(MAA-co-MAChol)s were prepared, and were further characterized by NMR, FTIR, GPC, DSC and dynamic contact angle testing instrument (DCAT). In aqueous media, spontaneous micellization of the synthesized diblock terpolymer amphiphiles were continuously examined by critical micellization concentration assay, DLS and TEM, and the efficacies of DOX loading by these copolymer micelles were investigated along with the complexed nanoparticle stability. Furthermore, *in vitro* DOX release of the drug-loaded terpolymer micelles were studied at 37 ^{o}C in buffer under various pH conditions, and cell toxicities of as-synthesized diblock amphiphiles were examined by MTT assay. At last, with H1299 cells, intracellular DOX delivery and localization by the block amphiphile vectors were investigated by invert fluorescence microscopy. As a result, it was revealed that the random copolymerization of MAA and MAChol comonomers in the second block limited the formation of cholesterol liquid-crystal phase, and enhanced DOX loading efficiency and complex nanoparticle stability, and that ionic interactions between the DOX and MAA comonomer could be exploited to trigger efficient DOX release under acidic condition, and the diblock terpolymer micellular vector could alter the DOX

trafficking in cells. Hence, these suggest the pH-sensitive PMAgala-*b*-P(MAA-*co*-MAChol)s might be further exploited as a smart nano-platform toward efficient anti-tumor drug delivery.

KEYWORDS

Terpolymer Amphiphiles; Galactose; Cholesterol; pH-responsive; Doxorubicin; Delivery

INTRODUCTION

In the recent decades, synthetic glycopolymers with saccharide grafts such as galactose (GAL), mannose (MAN), lactobionic acid (LBA) and so forth have attracted broad interests. It provides a great potential toward advanced drug/gene delivery, tissue engineering, organ regeneration as well as clinical diagnostics and biomedical imaging.[1–4] Up to date, it has already been uncovered that the bioactive GAL and LBA grafts could give rise to favorable water-solubility instead of polyethylene glycol (PEG). In addition, they have strong and specific binding to the asialoglycoprotein receptors (ASGPR), which is over-expressed on human hepatocyte surface.[5] Therefore, the GALs and/or LBAs have been extensively exploited as potent blocks in designing translocating vectors for drug delivery systems targeting human liver cancer cells.[6–8] For instance, two series of diblock P(MEO_2MA-*co*-OEGMA)-*b*-PMAGP and P(MAGP-*co*-DMAEMA)-*b*-PPDSMA copolymer amphiphiles with GAL grafts were prepared by Pan et al.[9,10], and their self-assembled supramolecular nanoparticles could be uptaken by HepG2 cells in a more efficient way than HeLa cells. Amphiphilic sugar-functional polycarbonate micelles also exhibit strong ability targeting HepG2 cells *in vitro*[11]. Alternatively, Ahmed et al.[12] explored the hemocompatibility of hyperbranched glycopolymers, and thereby convinced the presence of these glycopolymers would not lead to clot formation, red blood cell aggregation and any immune response. Taking the advantages of LBAs and reduction-responsive disulfide linkages

into account, glyco-nanoparticles have been reported to bear reduction-sensitive sheddable LBA shells as potent hepatoma-targeting anticancer drug delivery vectors[13]. Likewise, polymeric gene vectors bearing mannitols and some other saccharides have also been revealed to be able to stimulate glyco-nanoparticle cellular uptake and trafficking via selectively activated endocytic and intracellular trafficking gateways.[14,15] Moreover, Yang et al.[16] recently uncovered that two factors of enhanced permeability-and-retention effect (EPR) and lectin-mediated hepatoma-targeting ability simultaneously influenced the doxorubicin (DOX) delivery *in vivo* by biodegradable polycarbonate micellar nanoparticles with GAL surface grafts. Since a PEG with its molecular weight higher than 40 KDa may encounter the metabolic issue of accumulation in tissues and organs[17], alternative hydrophilic polymers bearing the saccharides like GAL and LBA have been expected with stealth effect and biological functions.

On the other hand, cholesterol as an essential component of the plasma membrane, has been known to be involved in many cellular processes such as membrane property regulation, steroidogenesis, bile acid synthesis and cellular signal transduction.[18,19] Meanwhile, a Niemann-Pick C1-like transmembrane protein (NPC1) mediates its intracellular uptake and transportation in living cells,[20] and the cholesterols translocate through lysosome-peroxisome membrane contacts[19]. As for its potential application in drug delivery, cholesterols attached onto the N-(2-hydroxypropyl) methacrylamide (HPMA)-based copolymer drug conjugates could result in lowered blood clearance and enhanced accumulation in tumors than their dodecyl or oleic acid conjugated counterparts[21], and the strong hydrophobic interactions between the cholesterols and anticancer drugs played crucial roles in enhancing paclitaxel (PTX) drug loading levels[22]. Notably, the cholesterol conjugates of amphiphilic copolymer vectors were further found to be capable of altering the DOX-loaded complex nanoparticle cellular

internalization mechanism[23]. In addition, cholesterol as an interesting natural rod-like mesogen has recently been explored for the structural design of new liquid crystalline (LC) organics, functional synthetic lipids and linear-dendritic block LC copolymers.[24–27] In particular, tailored block structural LC copolymer amphiphiles bearing grafted cholesterols like poly(ethylene glycol)-*b*-poly(cholesteryl acryloyoxy ethyl carbonate)s, poly(6-cholesteryloxyhexyl methacrylate)-*b*-poly(2-hydroxyethyl methacrylate)s and poly(glyceryl methacrylate)-*b*-poly(6-cholesteryloxyhexyl methacrylate)s were found to self-assemble in aqueous media into nano-objects with finely ordered hierarchical structures due to the cholesterol hydrophobic interactions and mesogen stacking, and a number of unique morphologies as periodically layered rod-like micelles, ellipsoidal vesicles, solid spheres and nano-tubes have been disclosed.[28–33] Moreover, Lu et al.[34] and Li et al.[35] separately prepared amphiphilic graft copolymers and reduction-sensitive diblock copolymers bearing pendant cholesterols, and their self-assembled nanoparticles and vesicles were further explored for DOX and calcein release, respectively. However, challenges of slow and less responsive release in cells still remained, which were due to the strong cholesterol hydrophobic interaction and highly ordered solid LC phase structure, and these impede their practical application as efficient drug delivery vectors.

As for a polymeric micellar drug vector, utilizing cholesterol grafts seems to be very helpful for decreasing drug leakage and initial burst release, and enhancing micelle stability under infinite dilution via physical cross-linking by cholesterol interactions[27,35]. To further realize the controlled drug release by the cholesterol-based copolymer amphiphiles, additional responsive constituents seem to be important for triggering the efficient drug release. It has been known that human tumors exhibit feature acidicity of pH=6.5~7.2, and intracellular organelles like early-endosome and late-lysosome tend to be more acidic with pH=5~6 and 4~5, respectively.[36]

Therefore, these pH differences have thus been extensively exploited for rational design of pH-responsive drug release carriers.[37, 38] The methacrylic acid (MAA) monomer has a pK_a of 5~6,[39] and the presence of biocompatible MAA comonomers in amphiphilic copolymers could enhance the interactions between the copolymer carriers and doxorubicins (DOX) through strong ionic interactions under physiological condition, ultimately leading to efficient drug loading.[40–42] Taking the advantages of MAA, galactose and cholesterol mesogen into account, in this work, we first designed and prepared a new series of amphiphilic diblock terpolymer poly(6-*O*-methacryloyl-D-galactopyranose)-*b*-poly(methacrylic acid-*co*-6-cholesteryloxyhexyl methacrylate)s hereby denoted as PMAgala-*b*-P(MAA-*co*-MAChol) via RAFT copolymerization, and molecular structures of as-synthesized diblock terpolymers were further characterized by means of NMR, FTIR and GPC. Then, the PMAgala-*b*-P(MAA-*co*-MAChol) supramolecular nanoparticles with/without DOX drug payloads were examined in terms of drug loading efficiency, micellar particle morphologies and stability. Cytotoxicity of these prepared diblock terpolymer amphiphiles was evaluated by MTT assay with H1299 cells. Finally, *in vitro* DOX drug release and their intracellular delivery by the PMAgala-*b*-P(MAA-*co*-MAChol) vectors were examined and discussed.

EXPERIMENTAL SECTION

Materials

Cholesterol (97%), D-galactose (99%) and methacryloyl chloride (98%) were purchased from *Shanghai Sinopharm Chemical Reagent Co. Ltd* (*China*) and utilized as-received. N,N'-azobis (isobutyronitrile) (AIBN, 98%, *Shanghai Sinopharm Chemical Reagent Co. Ltd*) was recrystallized twice from methanol prior to use. Tert-butyl methacrylate (^{t}BMA, 99%, *Sigma & Aldrich*) was purified via basic alumina gel column chromatography. RAFT agent of

4-cyano-4-(dodecylsulfanyl thiocarbonyl) sulfany pentanoic acid (CDP) was prepared as referred to the literature[43]. 6-Cholesteryloxyhexyl methacrylate (MAChol) was synthesized and further purified as previously reported[29]. Toluene was refluxed over metallic sodium and distilled before use. Fluorescent probe of pyrene (95%) for CMC measurement was bought from *Aladdin Chemical Reagent Co. Ltd* (*China*). All other organics were commercially supplied and used as-received. In addition, cellulose dialysis membrane (MWCO 3500) was purchased from *Shanghai Green Bird Science & Technology Development Co. Ltd* (*China*). Doxorubicin (DOX, 98%) was purchased from *Zhejiang Hisun Pharmaceutical Co. Ltd* (*China*). Sodium dodecyl sulfate (SDS, 99%), fetal bovine serum (FBS, Cat#10099-141) and bovine serum albumin (BSA, Cat#0332) were purchased from *Genebase Gene Tech Co. Ltd* (*China*), *Invitrogen (USA)* and *Amresco (USA),* respectively. Thiazoyl blue tetrazolium bromide (MTT, Cat#M5655) was supplied by *Sigma & Aldrich (USA)*. PARP antibody (Cat#9542) was received from *Cell Signaling Technology, Inc* (*USA*). RPMI1640 (Cat#11875-093) and DMEM (Cat#11995-065) mediums were purchased from *GIBCO* (*USA*). β-tubulin antibody (Cat#MAN1003), sodium pyruvate solution (100X, Cat#MG6096), antibiotics penicillin (100 IU/mL) and streptomycin (100 μg/mL) (Cat#MG7989), L-glutamine (Cat#MG8042), horseradish peroxidase-linked rabbit anti-mouse immunoglobulin (Cat#MAN4001) and horseradish peroxidase-conjugated goat anti-mouse immunoglobulin G (Cat#MAN4002) were supplied by *MesGen (China)*. Chemiluminescence kit (Cat#34077) was purchased from *Pierce (USA)*. H1299 and HepG2 cell lines were kindly gifted by Dr. Bo Wan of Key Laboratory of Genetic Engineering of Fudan University (*Shanghai, China*).

Instrumental Characterization

NMR spectra Routine ^{1}H NMR spectra were recorded on a Varian-300 FT-NMR spectrometer operated at 300.0 MHz for proton nuclei, and ^{13}C NMR characterization was implemented on a Bruker Avance-400 FT-NMR spectrometer (100.0 MHz for ^{13}C nuclei) with $CDCl_3$ or DMSO-d_6 as the solvents. Measurements of NMR spectra were conducted at ambient temperature with tetramethylsilane (TMS) as internal chemical shift reference. In addition, temperature-resolved ^{1}H NMR spectra were recorded on a Bruker Avance-400 FT-NMR spectrometer (400.0 MHz for proton nuclei) with a BVT2000 temperature controller and pyridine-d_5 as the solvent.

Mass spectra ESI-MS were routinely measured on a Varian SATURN 2000 instrument.

FTIR spectra FTIR spectra were recorded on a Bio-Rad FTS-185 spectrometer at room temperature with 64 scans spanning a spectral range of 4000～500 cm^{-1} with a resolution of 4.0 cm^{-1}. Samples were first well-dissolved in an organic solvent (chloroform or pyridine), and then drop-casted on potassium bromide (KBr) pellets and dried prior to the measurement.

Elemental analysis Oxygen elemental analysis was routinely conducted on an Elementar vario EL Ⅲ system (*German*).

Gel permeation chromatography (GPC) Molecular weights (M_n, M_w) and polydispersity (M_w/M_n) of the synthesized polymers were routinely measured at 35°C on a PerkinElmer 200 GPC equipped with a refractive index detector (RI). THF was utilized as the eluent at a flowing rate of 1.0 mL/min, and polystyrene standards (*Polymer laboratories, UK*) were applied to calibrate the GPC traces.

Dynamic light scattering (DLS) Particle sizes and zeta potentials of the amphiphilic micelles were analyzed at 25°C or 37°C on a Malvern Zetasizer Nano ZS90 dynamic light scattering instrument with laser incident beam at λ=633 nm and a fixed scattering angle of 90°.

Transmission electronic microscopy (TEM) Micelle morphologies were investigated by TEM (JEOL-1230, *JEOL Co. Ltd, Japan*) with an acceleration voltage of 80 KV. Typically, micelle solution with a concentration of 1.0 mg/mL was dropped onto a 300-mesh carbon-coated copper grid, and excess fluid was removed with filter paper and finally air-dried at room temperature. The morphologies of the micelles were immediately observed without further stain.

Preparation of new amphiphilic diblock terpolymers

Synthesis of 6-O-Methacryloyl-1,2:3,4-di-O-isopropylidene-D-galactopyranose (MAIpGP) monomer MAIpGP was synthesized in a way as partially referred to the literatures[9,44]. In brief, D-galactose was protected via reacting with acetone in the presence of concentrated H_2SO_4 (98%) and anhydrous $CuSO_4$, and then esterified with methacryloyl chloride in ice bath. After purification via column chromatography, the MAIpGP products were collected as white solids (yield of two steps: 64%).

^{1}H NMR ($CDCl_3$, δ in ppm): 6.13 (m, 1H, =CH*H*), 5.58 (m, 1H, =C*H*H), 5.53 (d, 1H, Galactopyranose (Gal)−*H* at 1 position), 4.62 (m, 1H, Gal−*H* at 3 position), 4.30 (m, 4H, Gal−*H* at 2, 4 and 6 position), 4.05 (m, 1H, Gal−*H* at 5 position), 1.93 (s, 3H, C*H*$_3$CR=CH_2), 1.53-1.33 (m, 12H, (C*H*$_3$)$_2$COO).

^{13}C NMR ($CDCl_3$, δ in ppm): 167.2, 136.0, 125.8, 109.6, 108.8, 96.3, 71.1, 70.7, 70.5, 66.1, 63.6, 25.9, 25.0, 24.4, 18.3.

FTIR (in cm^{-1}): 2978, 2926, 1716, 1384, 1258, 1208, 1176, 1164, 1113, 1066, 1006, 936, 900, 865.

ESI-MS [$M+H^+$] (in m/z): 329.1 (*Calc.:* 329.2).

RAFT polymerization of MAIpGP Polymerization of MAIpGP monomer was conducted by controlled RAFT polymerization. Typically, MAIpGP (656.0 mg, 2.0 mmol), CDP (40.4 mg, 0.1

mmol) and AIBN (3.3 mg, 0.02 mmol) were dissolved in freshly distilled toluene (4.4 mL), and placed into a Schlenk tube equipped with magnetic stirrer. The mixture was deoxygenated by freeze-pump-thawing for three times, and then immersed into an oil bath thermostated at 80°C for 8 h. At predetermined time intervals, the reaction mixture was sampled by a syringe, and the monomer conversion and molecular weight were analyzed by ^{1}H NMR and GPC. The reaction was stopped by cooling in ice bath, and precipitated in cooled dry hexane, and the collected precipitates were dried under vacuum to finally obtain yellowish PMAIpGP powders.

^{1}H NMR ($CDCl_3$, δ in ppm): 5.53 (d, Gal−*H* at 1 position), 4.62 (m, Gal−*H* at 3 position), 4.35-3.90 (m, Gal−*H* at 2, 4, 5 and 6 position), 2.35 (s, HOOC*CH*$_2$R).

FTIR (in cm^{-1}): 2988, 2932, 1732, 1382, 1256, 1212, 1166, 1115, 1070, 1004, 892.

Synthesis of a series of diblock terpolymer PMAIpGP-b-P(^{t}*BMA-co-MAChol) precursors and final PMAgala-b-P(MAA-co-MAChol) amphiphiles* PMAIpGP-*b*-P(^{t}BMA-*co*-MAChol)s diblock terpolymers were prepared in a way similar to that for the PMAIpGP. In brief, predetermined amounts of PMAIpGP, AIBN, ^{t}BMA and MAChol dissolved in freshly distilled toluene were in turn added into a Schlenk tube with magnetic stirrer. After three cycles of freeze-pump-thawing, the Schlenk tube was immersed into an oil bath preheated at 80°C, and kept reaction for 16 h. After the precipitation for three times in anhydrous methanol, final yellowish powder terpolymer products were obtained after the drying under vacuum for 12 h. Furthermore, the as-prepared terpolymer precursors were deprotected at room temperature in mixed trifluoroacetic acid (TFA) and dichloromethane (DCM) (1/2, *v*/*v*) for 32 h, and PMAgala-*b*-P(MAA-*co*-MAChol) amphiphiles were prepared by repeated precipitation in anhydrous cold methanol and drying under vacuum .

PMAIpGP-b-P(^{t}*BMA-co-MAChol):*

^{1}H NMR ($CDCl_3$, δ in ppm): 5.53 (d, Gal−*H* at 1 position), 5.34 (d, =C*H*R of cholesterol), 4.65 (m, Gal−*H* at 3 position), 4.35-3.75 (m, Gal−*H* at 2, 4, 5 position and -CH_2COOR), 3.45 (t, CH_2OR of cholesterol), 3.12 (m, OC*H*R of cholesterol).

FTIR (in cm^{-1}): 2933, 2866, 1728, 1458, 1382, 1368, 1255, 1212, 1142, 1072, 1005.

PMAgala-b-P(MAA-co-MAChol):

^{1}H NMR (pyridine-d_5, 80°C, δ in ppm): 6.80-5.40 (Gal−*H* at 1 position and–O*H*), 5.54 (=C*H*R of cholesterol), 5.20-4.00 ppm (Gla-*H* at 2, 3, 4, 5 position and -CH_2COOR), 3.63 (CH_2OR of cholesterol), 3.35 (OC*H*R of cholesterol).

FTIR (in cm^{-1}): 3363, 2933, 2866, 1726, 1466, 1366, 1254, 1147, 1103.

Preparation of diblock terpolymer amphiphiles and their DOX-loaded micelles

The terpolymer amphiphiles and their DOX-loaded micelles were prepared in a way as following: In brief, 10.0 mg of each synthesized terpolymer amphiphile was first dissolved in 1 mL of THF/DMSO (1/1, *v/v*), and stirred at room temperature for 8 h. Then, 5 mL phosphate buffer (pH 7.4, 10 mM) was added dropwise into the mixture under vigorous stirring. The resultant solution was further dialyzed against deionized water for 48 h using a pre-swollen cellulose dialysis membrane (MWCO 3500) to remove residual solvent. In a similar way, DOX (10.0 mg) and triethylamine (TEA, 2 mol equiv. to DOX) were dissolved in 1 mL of DMSO, and stirred for 4 h, then 40.0 mg of terpolymer amphiphilie preliminarily dissolved in 4 mL of THF/DMSO (1/1, *v/v*) was again added. Afterwards, 20 mL of phosphate buffer (pH=7.4, 10 mM) was gradually placed into above mixture, and the DOX-loaded terpolymer amphiphilie micelle solution was dialyzed in deionized water for 48 h to give drug-loaded amphiphilie micelle aqueous solution. The DOX loading levels were accordingly measured by UV-Vis spectrophotometer (UV-2800, *Hitachi*, *Japan*). Lyophilized DOX-loaded terpolymer micelles

were dissolved in DMSO, and the DOX concentration was evaluated according to a standard curve, and DOX loading content (DLC) and loading efficiency (DLE) were further calculated according to the following formulas:[45]

$$\mathrm{DLC}(wt\%) = \frac{\text{Weight of loaded drug}}{\text{Weight of loaded drug and polymers}} \times 100\%$$

$$\mathrm{DLE}(\%) = \frac{\text{Weight of loaded drug}}{\text{Weight of drug in feed}} \times 100\%$$

Critical micelle concentration (CMC)

Pyrene was utilized as fluorescence probe to determine the CMC of as-synthesized terpolymer amphiphiles. Briefly, 10 μL of pyrene/acetone solution (1.2×10^{-4} M) was placed into the terpolymer micelle aqueous solution under various mass concentration of $1\times10^{-5}\sim5\times10^{-1}$ mg/mL to adjust final 6.0×10^{-7} M pyrene in micelle solution, then kept at room temperature in dark for 24 h before the measurement. Fluorescence spectra were recorded on a fluorescence spectrophotometer (F-7000, *Hitachi*, *Japan*) with an excitation wavelength of 334 nm and scanning wavelength of 350～450 nm, and fluorescence intensity ratios ($\boldsymbol{I}_{394}/\boldsymbol{I}_{374}$) were calculated, and plotted as a function of terpolymer concentration. The CMC for each terpolymer amphiphilie was routinely determined as ever reported[11].

Stability of DOX-loaded terpolymer micelles

Stability of the DOX-loaded terpolymer amphiphile micelles (1.0 mg/mL) was examined by DLS, and the SDS (100 μg/mL) was employed as a destabilizing agent[22], and light scattering intensity was continuously monitored by DLS at 37°C over a period of 48 h. Similarly, average particle sizes of the DOX-loaded micelles in the presence of 10% FBS, BSA (0.3%, m/v) and 2 M NaCl were separately analyzed after 24 h incubation.

DOX release in vitro

DOX release profiles were examined at 37°C under different pH for the drug loaded terpolymer amphiphile micelles in three kinds of media: (a) acetate buffer, pH=4.5, 10 mM; (b) phosphate buffer, pH=6.5, 10 mM; (c) phosphate buffer, pH=7.4, 10 mM. In brief, each DOX-loaded micelle solution (2.0 mg/mL, 3 mL) was placed into a cellulose dialysis membrane (MWCO 3500), and immersed into the above-mentioned media at 37°C under gentle shaking. At predetermined time intervals, 2 mL release media was sampled for UV-Vis analysis, and an equal volume of fresh media was added, and *in vitro* DOX release was routinely analyzed using a UV-Vis spectrophotometer[10].

MTT assays

Cytotoxicities of as-prepared terpolymer micelles were assayed with H1299 cells by MTT assay kit. Cells were first seeded into 96-well microplate (6×10^3 cells/well) with RPMI-1640 medium supplemented with 10% FBS, 1% L-glutamine, antibiotics penicillin (100 IU/mL) and streptomycin (100 μg/mL), and incubated for 24 h. Then, the medium was aspirated and replaced by 100 μL fresh medium with 10% FBS supplemented with micelle solution under various concentration of 0, 20, 50, 80 and 100 μg/mL, and kept cultivation at 37 °C under 5% CO_2 for another 30 h. Afterwards, 20 μL of MTT solution (5.0 mg/mL) was placed into the microplate replaced with 100 μL FBS-free fresh medium, and further incubated for another 2 h. 100 μL of DMSO was added into each well to dissolve the MTT-formazan, and light absorbances at λ=490 were measured on microplate reader (BioTek, ELX800) with λ=630 nm as the reference. As a result, relative cell viability was evaluated with n=5 as following:

Cell viability (%)=$(OD_{490(sample)}-OD_{630(sample)})/(OD_{490(control)}- OD_{630(control)})\times100\%$

In a similar way, cell viabilities were also examined for the DOX-loaded diblock terpolymer amphiphile micelles and free DOX with H1299 and HepG2 cell lines. As for the MTT assay with

HepG2 cell line, the HepG2 cells were first cultivated with DMEM medium supplemented with 10% FBS, 1% L-glutamine, antibiotics penicillin (100 IU/mL), streptomycin (100 μg/mL) and sodium pyruvate (1mM). After 24 h incubation, the medium was aspirated, and replaced by 100 μL fresh medium (with 10% FBS) supplemented with different amounts of DOX-loaded terpolymer micelles or free DOX to adjust final DOX concentration of 0.3, 1, 3, 5, 10 and 15 μg/mL, and kept incubation at 37°C under 5% CO_2 for 30 h. Thereafter, cell viability was thus assayed by the MTT assay kit.

Intracellular DOX release

Cellular uptake and intracellular DOX release of the DOX-loaded micelles and free DOX control were examined with H1299 cells on fluorescence microscopy. First, the cells were cultured on microscope slides in 6-well plate (5×10^5 cells/well) using RPMI-1640 medium with 10% FBS, 1% L-glutamine, antibiotics penicillin (100 IU/mL) and streptomycin (100 μg/mL), then the cells were incubated at 37°C with either DOX-loaded micelles or free DOX for 1 and 6 h. After the removal of culture medium, the cells were rinsed three times with 1×PBS, and stained cell nuclei with Hoechst 33342, then fluorescence images were recorded on Nikon Ti-S invert fluorescence microscopy.

Western-blot assay

H1299 cells preliminarily treated with either free DOX or DOX-loaded micelles for 30 h were harvested and extracted with RIPA lysis buffer, and then incubated at 95°C for 15 min. Total protein was separated by 8% SDS-PAGE, and blotted to nitrocellulose transfer membranes. The membranes were further blocked with 3% BAS TBST (20 mM Tris–HCl, pH 7.6, 137 mM NaCl, and 0.01% Tween-20) for 1 h at the room temperature, followed by incubation with PARP or β-tubulin primary antibodies at 4°C over night. After extensive washing with TBST, the

membranes were allowed to be reprobed with horseradish peroxidase-linked anti-mouse immunoglobulin in 5% BSA TBST for 40 min, and unreacted antibodies were separated with TBST for three times. Then, the membranes were subjected to western-blot analysis with the signals from the primary antibody amplified by horseradish peroxidase-conjugated goat anti-mouse immunoglobulin G. Finally, the protein bands were detected and recorded by a chemiluminescence kit.

RESULTS AND DISCUSSION

Synthesis and Characterization of Diblock Terpolymer PMAgala-b-P(MAA-co-MAChol)s

As for the preparation of functional glycopolymers, controlled radical polymerization has been widely employed as an effective synthetic approach.[46] Lowe et al[47] reported the first RAFT polymerization of 6-*O*-methacryloyl-1,2:3,4-di-*O*-isopropylidene-D-galactopyranose (MAIpGP) monomer, and several dithiobenzoate-type chain transfer agents (CTAs) have been explored in the MAIpGP RAFT polymerization.[9,10,44] In this work, as shown in Scheme 1, the monomers of MAIpGP and MAChol were accordingly synthesized with good yields. Figures 1A and 1B depict ^{1}H NMR spectra for the MAIpGP and MAChol monomers, and the resonance signals were accordingly assigned[9,29]. Furthermore, the PMAIpGP was prepared under an optimized reaction temperature of 80ºC in toluene through RAFT polymerization with AIBN and the synthesized 4-cyano-4-(dodecylsulfanylthiocarbonyl) sulfany pentanoic acid (CDP) as the initiator and CTA, respectively, and the initial CTA/initiator molar ratios were hereby optimized to be 1/0.2.[10] Figure 2A presents ^{1}H NMR spectrum of the PMAIpGP product, and the ^{1}H resonance signals (*a*, *h*) could be assigned to the ^{1}H nuclei neighboring anomeric carbon in sugar ring and methylene group of the CTA moiety, demonstrating successful RAFT polymerization. To make more clear the MAIpGP RAFT polymerization kinetics, Figure 3 shows the results of polymerization

kinetics study at 80°C in toluene under a MAIpGP/CDP/AIBN molar ratio of 20/1/0.2, and the $Ln([M]_0/[M]_t)$ *vs* reaction time (*t*) plots as seen in Figure 3A tend to exhibit a good linear relationship, inferring a pseudo-first order polymerization kinetics for the MAIpGP monomer. Moreover, Figure 3B shows the MAIpGP monomer conversion dependence of number average molecular weight (M_n) by GPC, indicating a linear relationship with polydispersity indices (M_w/M_n) lower than 1.2, demonstrating controlled polymerization of the PMAIpGP.

To achieve amphiphilic diblock terpolymer PMAgala-*b*-P(MAA-*co*-MAChol)s, the purified PMAIpGP were continuously employed as the macro-RAFT agents for successive random copolymerization of MAChol and ^{t}BMA comonomers at 80°C in toluene to give PMAIpGP-*b*-P(^{t}BMA-*co*-MAChol) precursors as shown in Scheme 1C, and Figure S1 depicts a copolymerization time dependence of the MAChol and ^{t}BMA comonomer conversion under an initial MAChol/^{t}BMA/macro-RAFT/AIBN feeding molar ratio of 15/25/1/0.2, and the observed similar consumption rates for these two comonomers may indicate the occurrence of random RAFT copolymerization of the second block. The resulted random comonomer sequence may be helpful for tuning the interactions and ordering of cholesterol mesogens and successive physical cross-linking of PMAgala-*b*-P(MAA-*co*-MAChol) micelles[34,35]. Figure 2B shows typical ^{1}H NMR spectrum for as-resulted PMAIpGP-*b*-P(^{t}BMA-*co*-MAChol), and GPC traces of the PMAIpGP macro-RAFT agent and as-synthesized series of diblock terpolymers are presented in Figure 4. In general, Table 1 summarizes synthetic results for the PMAIpGP macro-RAFT agent and PMAIpGP-*b*-P(^{t}BMA-*co*-MAChol)s, and the assigned ^{1}H NMR resonance signals and high monomer conversions as well as low M_w/M_n values substantiated successful preparation of the $PMAIpGP_{18}$-*b*-P(^{t}BMA-*co*-MAChol) precursors with narrow molecular weight distribution.

So far, trifluoroacetic acid (TFA) has already been known as a standard reagent to remove the *tert*-butyl and isopropylidene groups of protected galactoses, and has been reported to have less influence on the other type of ester structures and cholesterol skeleton.[47-49] In this work, a reaction conditions of TFA/DCM (1/2, *v*/*v*) for 32 h was employed to deprotect the terpolymer PMAIpGP$_{18}$-*b*-P(^{t}BMA-*co*-MAChol) precursors. Figure S2C depicts FTIR spectra for the PMAIpGP$_{18}$-*b*-P(^{t}BMA$_{16}$-*co*-MAChol$_{12}$) and achieved diblock terpolymer amphiphile product, and remarkable new emergence of broad IR absorption around 3300 cm^{-1} assignable to *–OH* stretch vibration of the resulted terpolymer amphiphile could be observed, indicating efficient *tert*-butyl and isopropylidene removals. Since the PMAgala-*b*-P(MAA-*co*-MAChol) terpolymer amphiphiles could not be well dissolved at the room temperature in the most of commonly used deuterated solvent, temperature-resolved ^{1}H NMR spectra with pyridine-d_5 solvent were recorded as shown in Figure S3, and the conditions of pyridine-d_5 solvent at 80°C was used to record ^{1}H NMR spectrum with better resolution for the PMAgala$_{18}$-*b*-P(MAA$_{16}$-*co*-MAChol$_{12}$) as shown in Figure 2C. The theoretical and experimental resonance intensity ratios of the ^{1}H signals at δ=3.55~3.75 ppm (-C*H*$_2$-O-CHR$_2$ of cholesterol grafts) to those at δ=4.00~5.20 ppm (-C*H*$_2$COO- and the Gla-*H* at 2, 3, 4, 5 position) were estimated to be 1/5.50 and 1/5.13, respectively. As a result, the galactose graft preservation could further be estimated to reach 91.7%. Since the ^{1}H resonance signals of *tert*-butyl and isopropylidene groups around δ=1.38~1.48 ppm overlapped with the signals of cholesterol skeleton, to give a deep insight into the deprotection of diblock terpolymer precursors, additional diblock copolymer analogues of PMAIpGP$_{18}$-*b*-P^{t}BMA$_{18}$ and their deprotected PMAgala$_{18}$-*b*-PMAA$_{18}$ were synthesized, and ^{1}H NMR spectra of the PMAIpGP$_{18}$-*b*-P^{t}BMA$_{18}$ in $CDCl_3$ and PMAgala$_{18}$-*b*-PMAA$_{18}$ in DMSO-d_6 are depicted in Figures S2A and S2B. It could be clearly seen that after the deprotection in TFA/DCM, ^{1}H

resonance signals at δ=1.40~1.47 ppm attributable to the *tert*-butyl and isopropylidene thoroughly disappeared, demonstrating efficient TFA-catalyzed removal of protecting groups. Furthermore, oxygen elemental analysis for the diblock terpolymer $PMAIpGP_{18}$-*b*-P($^{t}BMA_{16}$-*co*-$MAChol_{12}$) precursor and $PMAgala_{18}$-*b*-P(MAA_{16}-*co*-$MAChol_{12}$) amphiphile were conducted with the resulted oxygen elemental percentages of 19.88% and 23.41%, respectively, which agrees well with their corresponding theoretical values of 20.40% and 24.53% within the instrumental limit. Hence, the experimental evidences of ^{1}H NMR and oxygen elemental analysis substantiate efficient deprotection with negligible cleavage of cholesterol/galactose grafts.

Furthermore, Figure S4 presents the recorded pictures of water-droplets on the thin film surfaces of as-synthesized series of diblock terpolymer amphiphiles, and the calculated contact angles tend to decrease from 106.4±1.3°, 104.3±0.9°, 100.2±2.1° to 93.0±2.5° with increasing MAA comonomer content, demonstrating the more hydrophilic physical properties. As for their thermal properties, thermostated polarized optical microscopic (POM) pictures and temperature modulated DSC traces are shown in Figures S5 and S6A, respectively. $PMAChol_{18}$ homopolymer prepared by similar RAFT polymerization was observed to show feature fan-type texture of smectic A (SmA_d) LC phase as previously reported[33,50], and glass transition temperatures (T_g) of the prepared diblock terpolymer amphiphiles were evaluated to increase from 27.7°C, 42.0°C, 46.0°C to 54.9°C along with increasing MAA comonomer content. Since the MAA repeating units are ionic comonomers, the phenomena of T_g increase in DSC traces for the terpolymer amphiphiles with more MAA units could be interpreted for their strong hydrogen bonding and ionic interactions in between[51]. Moreover, no obvious liquid crystal phase transition was observed for the above-synthesized copolymers during the DSC cooling and heating scans

(Figure S6B and S6C). These results may be accounted for the disturbed cholesterol stacking due to the presence of MAA comonomers in vicinity, and this would be beneficial for tuning micellar physical cross-linking, DOX loading and intracellular drug release as discussed below.

Preparation of DOX-loaded Supramolecular Micelles by the PMAgala-b-P(MAA-co-MAChol)s

To further exploit above-synthesized PMAgala-*b*-P(MAA-*co*-MAChol)s as potential DOX delivery vectors, their CMC in aqueous media were measured with pyrene as the fluorescent probe as shown in Figure S7, and very low CMC were calculated to be 1.41~2.82 mg/L for the $PMAgala_{18}$-*b*-$PMAChol_{14}$ and the series of $PMAgala_{18}$-*b*-P(MAA-*co*-MAChol)s as summarized in Table 2, and these results suggest strong hydrophobic association of cholesterol grafts, which seems favorable for high micelle stability against extreme dilution during blood circulation *in vivo*.[52] Figure 5 depicts particle sizes and morphologies of the $PMAgala_{18}$-*b*-P(MAA_{26}-*co*-$MAChol_9$) micelles characterized by DLS and TEM, respectively, and monodisperse spherical micelles could be observed by TEM with an average particle size of 40.3 nm, which is smaller than 94.9 nm in wet state by DLS due to the micelle shrinkage upon dehydration.[10] In general, Table 2 summarized the micelle sizes for the $PMAgala_{18}$-*b*-$PMAChol_{14}$ and the series of $PMAgala_{18}$-*b*-P(MAA-*co*-MAChol)s, and the micelles with particle sizes of 48.9~140.2 nm formed, strongly depending on their copolymer comonomer composition. Herein, it is noteworthy that under physiological environment, larger size terpolymer micelles could be observed for the $PMAgala_{18}$-*b*-P(MAA-*co*-MAChol)s with higher MAA comonomer contents, and this could be interpreted for the increased hydrophilicity and negative charge repulsion of the carboxyl grafts.

In contrast, the DOX-loaded $PMAgala_{18}$-*b*-$PMAChol_{14}$ and $PMAgala_{18}$-*b*-P(MAA-*co*-

MAChol)s complex micelles showed particle sizes, decreasing from 243.9 nm to 95.8 nm with increasing the MAA comonomer contents, and the drug-loaded diblock terpolymer micelles with particle sizes smaller than 200 nm seem favorable for being accumulated in tumor vasculature via EPR.[53] Concerning the decrease in micelle particle size for the amphiphilic terpolymers with more MAA comonomer, it could be accounted for the reasons that after drug loading under neutral condition, positively charged DOX (pK_a=8.2)[54] would interact with negatively charged MAA carboxyl groups (pK_a=5~6), and the charge neutralization would further decrease their water-solubility and give rise to more compacted solid micelles with decreased particle sizes and enhanced complexed micelle stability. Moreover, as seen in Table 2, under neutral condition, all DOX-loaded micelles showed zeta-potentials of -12.2 to -26.9 mV, and the negative surface charge may prevent their interactions with serum proteins, and thus be favorable for long circulation *in vivo*.[55] Moreover, π-π-stacking, electrostatic interaction and hydrogen bonding between the polymer and drug have been well harnessed to increase drug loading efficiency and micelle stability.[56,57] In a view of drug loading efficacy (DLE) for the PMAgala$_{18}$-*b*-PMAChol$_{14}$ and PMAgala$_{18}$-*b*-P(MAA-*co*-MAChol)s micelles, the incorporation of a third MAA comonomer led to remarkably increased DLE from 47.1% to 91.2%, demonstrating that the cholesterol and MAA could synergistically improve the DOX encapsulation. As for the copolymer amphiphiles bearing cholesterols, it has been known that the cholesterols in micellar core could result in high drug loading due to hydrophobic interactions between the cholesterols and drugs[22,58], however, the cholesterols could also spontaneously form cholesterol LC phase, and thus decrease their interactions with drug molecules[22]. On the evidences of DOX loading by the synthesized diblock terpolymer PMAgala$_{18}$-*b*-P(MAA-*co*-MAChol)s, it could be demonstrated that hydrophobic association and ionic interaction between the MAA comonomer carboxyl and DOX significantly

enhanced DOX loading for the diblock terpolymers, and random comonomer sequences in the second block limited cholesterol LC phase formation as evidenced in Figure S5B and S5C.

Figure 6 presents stability assay results of the DOX-loaded complex micelles in aqueous media by DLS with SDS destabilizing agent (100 μg/mL) as referred[59]. It could be seen that the light intensity of diblock PMAgala$_{18}$-*b*-PMAChol$_{14}$/DOX micelle solution dropped down to 75% within 48 h after adding SDS, while the DOX-loaded complex micelles by three PMAgala$_{18}$-*b*-P(MAA-*co*-MAChol)s showed excellent stability against SDS. Meanwhile, no significant particle size change was observed after incubating PMAgala$_{18}$-*b*-P(MAA$_{26}$-*co*-MAChol$_9$)/DOX micelles under 2 M NaCl or 0.3% (m/v) BSA, and only slight swelling could be detected in 24 h with 10% FBS. These results inferred that the copolymerization of MAChol and MAA comonomers as the second block endowed excellent stability of DOX-loaded micelles.

Responsive DOX Release of Drug Loaded Diblock Terpolymer Micelles

Figure 7 depicts pH dependence of particle sizes for the DOX-loaded diblock terpolymer PMAgala$_{18}$-*b*-P(MAA$_{26}$-*co*-MAChol$_9$) micelles at 37°C in buffer solution by DLS. It could be seen that in acetate buffer (pH=4.5), the initial terpolymer micelle size was around 90~100 nm, and the micelle sizes gradually increased along with the incubation time (0.5~16 h), and finally dual dispersive peaks respectively centering around 120 nm and 1000 nm were detected due to the destruction and aggregation of the DOX-loaded complex micelles.[60] In contrast, after 24 h incubation in PBS buffer (pH=7.4), the DOX-loaded PMAgala$_{18}$-*b*-P(MAA$_{26}$-*co*-MAChol$_9$) micelles were just slightly swelled. Therefore, these results demonstrate strong pH dependence of the drug-loaded terpolymer micelle sizes. Figure 8 shows *in vitro* DOX release profiles by the diblock PMAgala$_{18}$-*b*-PMAChol$_{14}$ and diblock terpolymer PMAgala$_{18}$-*b*-P(MAA-*co*-MAChol)s

in various media. At pH=7.4, the drug slowly released, and only 7% DOX were released from the drug-loaded PMAgala$_{18}$-*b*-P(MAA$_{26}$-*co*-MAChol$_9$) micelles, in comparison no more than 30% DOX were released from the diblock PMAgala$_{18}$-*b*-PMAChol$_{14}$ micelles, this may infer that the copolymerization of MAA comonomer could not only stabilize the DOX-loaded terpolymer micelles, but also limit the DOX release at pH=7.4. At pH=6.5, the DOX release obviously accelerated, and cumulative drug release could reach 30~47% within 50 h. When pH was further decreased to 4.5, very fast and high cumulative DOX release could be observed for the amphiphilic drug carriers of PMAgala$_{18}$-*b*-PMAChol$_{14}$ (57.7%), PMAgala$_{18}$-*b*-P(MMA$_5$-*co*-MAChol$_{14}$) (78.0%), PMAgala$_{18}$-*b*-P(MAA$_{16}$-*co*-MAChol$_{12}$) (75.0%) and PMAgala$_{18}$-*b*-P(MAA$_{26}$-*co*-MAChol$_9$) (90.3%), respectively. These results might be interpreted for the facts that under pH condition below the pKa (5~6) of MAA carboxyl groups, ionic interactions between the encapsulated DOX and MAA comonomers in amphiphile micelle cores were significantly weakened while water-solubility of the DOX molecules simultaneously increased due to the protonation of amino groups, and these finally led to responsive terpolymer micelle disassembly and fast DOX releases under the acidic environment.

Cell Viability Assay and Intracellular DOX Delivery by PMAgala-b-P(MAA-co-MAChol) Micelles

Continuously, cell toxicities of as-prepared diblock PMAgala$_{18}$-*b*-PMAChol$_{14}$ and the series of terpolymer PMAgala$_{18}$-*b*-P(MAA-*co*-MAChol)s were assayed with human lung cancer H1299 cells, and the MTT assay results are shown in Figure S8. After 30 h incubation, negligible slight MTT toxicity could be observed under the amphiphile mass concentration up to 100 μg/mL, indicating excellent biocompatibility of the as-prepared terpolymer amphiphiles. Since the terpolymer PMAgala$_{18}$-*b*-P(MAA$_{26}$-*co*-MAChol$_9$) has shown highly efficient DOX loading and

pH responsive release, its DOX-loaded micelles were further employed to examine their cancer cell proliferation inhibition and intracellular DOX delivery. Figure 9 depicts H1299 and HepG2 cell viabilities after 30 h incubation in the presence of the PMAgala$_{18}$-*b*-P(MAA$_{26}$-*co*-MAChol$_9$)/DOX micelles and free DOX under a series of DOX dosages. It could be seen that the presence of either DOX-loaded terpolymer micelles or free DOX unambiguously resulted in DOX-dosage dependent cell viability, and relatively lower tumor cell inhibition exhibited for the DOX-loaded terpolymer micelles under the same DOX dosage in both cell lines. The IC_{50} values (half maximal inhibitory concentration) of DOX-loaded micelles were 13.34 μg DOX euqiv/mL and 8.58 μg DOX euqiv/mL toward H1299 cell line and HepG2 cell line, respectively, which are both higher than that of free DOX (6.74 μg/mL toward H1299 cell line and 6.67 μg/mL toward HepG2 cell line, respectively). This results indicated that the DOX-loaded complex micelles could be uptaken efficiently and release DOX in both H1299 and HepG2 cells, and the relatively lower tumor cell inhibition properties might be due to their different endocytic mechanisms as compared with free DOX and prolonged DOX release from the complex micelles as indicated in the *in vitro* DOX release profiles (Figure 8).[61,62] Furthermore, since H1299 cells generally have the merits of easy morphology observation with good reproducibility during cell biological study, thus H1299 cells were chosen to give further insights into the DOX endocytosis and intracellular trafficking. As shown in Figure 10, for the free DOX, after 1 h incubation, strong red DOX fluorescence could be observed predominantly in cell nuclei, and the fluorescence intensity localized in the cell nuclei was found to become stronger after 6 h incubation. This may be due to fact that the DOX small molecules could freely penetrate through plasma membrane via fast diffusion and rapid intracellular traffic to cell nuclei. As for the DOX-loaded diblock terpolymer micelles, red DOX fluorescence was predominantly observed in cytoplasm after 1 h incubation,

and significant DOX accumulation in cell nuclei could be seen after 6 h incubation, inferring that the DOX-loaded terpolymer micelles may be internalized into cells via endocytosis, and further release DOX in cytoplasm, and then deliver DOX into cell nuclei. These evidences are well consistent with the results of cell viability assay shown in Figure 9A and similar results as reported in literature[56].

Alternatively, it has already been known that the DOX is a topoisomerase□inhibitor which could cause DNA damage and cancer cell inhibition mainly by apoptosis. PARP, a 116 kDa nuclear poly(ADP-ribose) polymerase, has been known to be involved in DNA repair in response to environmental stress[63], and it is one of the main cleavage targets of caspase-3 *in vivo*[64]. The PARP cleavage occurs between Asp214 and Gly215, which could separate the PARP N-terminal DNA binding domain (24 kDa) from the C-terminal catalytic domain (89 kDa)[64], and the cleavage of PARP would facilitate cellular disassembly and serve as a marker of cells undergoing apoptosis[65]. Figure 11 shows H1299 cell morphological images (A~C) recorded by bright-field microscopy with free DOX as the control, and obvious cell growth inhibition could be observed after the incubation for 30 h under a fixed DOX dosage of 10 μg/mL for the free DOX and DOX-loaded diblock terpolymer micelles. Moreover, Figure 11D presents the western blot analytic results for the cells treated with either free DOX or DOX-loaded terpolymer micelles, and notably up-regulated PARP cleavages could be clearly observed with β-tubulin as the internal reference, demonstrating the apoptosis of H1299 cells in the presence of either free DOX or DOX-loaded terpolymer micelles. The western-blot experimental evidences indicate that the DOX delivered by the diblock terpolymer complex micelles could effectively result in cell apoptosis despite possible different trafficking routes of free DOX and DOX-loaded terpolymer complex micelles. Therefore, these infer that new diblock terpolymer micelles with efficient

DOX loading and pH-responsive drug release may be further developed as future drug delivery carriers as shown in Scheme 2, and continuous studies concerning liver cancer cell targeting and DOX-loaded complex particle autophagy in cells are now ongoing in this lab.

CONCLUSION

In this study, we designed and successfully synthesized a series of amphiphilic diblock terpolymer PMAgala-*b*-P(MAA-*co*-MAChol)s with side-attached galactose and cholesterol grafts. Structural and physical characterization demonstrated controlled RAFT copolymerization of the diblock terpolymers, and random copolymerization of the MAA and MAChol in the second block limited the formation of cholesterol LC phase, and the diblock terpolymers exhibited increased water-solubility when increasing their MAA comonomer composition. In aqueous solution, the PMAgala$_{18}$-*b*-PMAChol$_{14}$ and PMAgala$_{18}$-*b*-P(MAA-*co*-MAChol)s could self-assemble into micelles, and the diblock terpolymers could more efficiently encapsulate DOX with a DLE up to 91.2% with better complex micelle stability. *In vitro* DOX release profiles demonstrated high stability of the DOX-loaded terpolymer micelles under neutral condition, and significantly fast responsive DOX release with cumulative release up to 90.3% could be observed, and the higher MAA content of a diblock terpolymer tended to result in higher cumulative DOX release, strongly depending on the pH of buffer solution. MTT assay with H1299 cells indicated slight cytotoxicity of the PMAgala$_{18}$-*b*-PMAChol$_{14}$ and PMAgala$_{18}$-*b*-P(MAA-*co*-MAChol)s. The results of fluorescence microscopy revealed that the DOX encapsulated in the synthesized diblock terpolymer PMAgala$_{18}$-*b*-P(MAA$_{26}$-*co*-MAChol$_9$)/DOX micelles could be uptaken and delivered into cell nuclei in an efficient way, and their intracellular trafficking pathway may be altered as compared with the free DOX control. In addition, western-blot assay of the PARP biomarker indicated efficient apoptosis of H1299 cells

by the PMAgala$_{18}$-*b*-P(MAA$_{26}$-*co*-MAChol$_9$)/DOX micelles similarly as DOX control. Taking advantages of the DOX-loaded PMAgala-*b*-P(MAA-*co*-MAChol) micelles, these diblock terpolymers may be anticipated as potent vectors for controlled drug delivery *in vivo*.

ASSOCIATED CONTENT

Supporting Information Synthesis and ^{1}H NMR spectra of diblock PMAIpGP$_{18}$-*b*-P^{t}BMA$_{18}$ and PMAgala$_{18}$-*b*-PMAA$_{18}$, FTIR spectra of diblock terpolymer PMAIpGP$_{18}$-*b*-P(^{t}BMA$_{16}$-*co*-MAChol$_{12}$) and PMAgala$_{18}$-*b*-P(MAA$_{16}$-*co*-MAChol$_{12}$), temperature-resolved ^{1}H NMR spectra of the PMAgala$_{18}$-*b*-P(MAA$_{16}$-*co*-MAChol$_{12}$) amphiphile in pyridine-d_5, kinetic plots of RAFT polymerization of MAChol and ^{t}BMA comonomers, POM images of the PMAChol$_{18}$ homopolymer, images of water contact angle, temperature-modulated DSC and routine DSC curves and CMC plots of as-prepared copolymer amphiphiles, cell viability assay of copolymer micelles. This material is available free of charge via the Internet at *http://pubs.acs.org*.

AUTHOR INFORMATION

Corresponding Author

*E-mail: acao@ sioc.ac.cn

Author Contributions

The manuscript was written through contributions of all authors. All authors have given approval to the final version of the manuscript.

ACKNOWLEDGMENT

The authors are grateful to the financial supports partially from National Natural Science Foundation of China (21174160, 21002116 and 21372251).

REFERENCES

(1) Kiessling, L. L.; Grim, J. C. *Chem. Soc. Rev.* **2013**, *42*, 4476–4491.

(2) Li, X.; Chen, G. *Polym. Chem.* **2015**, *6*, 1417–1430.

(3) Narla, S. N.; Nie, H.; Li, Y.; Sun, X. *J. Carbohydr. Chem.* **2012**, *31*, 67–92.

(4) Spain, S. G.; Cameron, N. R. *Polym. Chem.* **2011**, *2*, 60–68.

(5) Mamidyala, S. K.; Dutta, S.; Chrunyk, B. A.; Préville, C.; Wang, H.; Withka, J. M.; McColl, A.; Subashi, T. A.; Hawrylik, S. J.; Griffor, M. C.; Kim, S.; Pfefferkorn, J. A.; Price, D. A.; Menhaji-Klotz, E.; Mascitti, V.; Finn, M. G. *J. Am. Chem. Soc.* **2012**, *134*, 1978–1981.

(6) Kawakami, S.; Hashida, M. *J. Control. Release* **2014**, *190*, 542–555.

(7) D'Souza, A. A.; Devarajan, P. V. *J. Control. Release* **2015**, *203*, 126–139.

(8) Zhong, Y.; Meng, F.; Deng, C.; Zhong, Z. *Biomacromolecules* **2014**, *15*, 1955–1969.

(9) Wang, Y.; Li, X.; Hong, C.; Pan, C. *J. Polym. Sci. Part A Polym. Chem.* **2011**, *49*, 3280–3290.

(10) Wang, Y.; Hong, C.; Pan, C. *Biomacromolecules* **2013**, *14*, 1444–1451.

(11) Suriano, F.; Pratt, R.; Tan, J. P. K.; Wiradharma, N.; Nelson, A.; Yang, Y. Y.; Dubois, P.; Hedrick, J. L. *Biomaterials* **2010**, *31*, 2637–2645.

(12) Ahmed, M.; Lai, B. F. L.; Kizhakkedathu, J. N.; Narain, R. *Bioconjug. Chem.* **2012**, *23*, 1050–1058.

(13) Chen, W.; Zou, Y.; Meng, F.; Cheng, R.; Deng, C.; Feijen, J.; Zhong, Z. *Biomacromolecules* **2014**, *15*, 900–907.

(14) Park, T.-E.; Kang, B.; Kim, Y.-K.; Zhang, Q.; Lee, W.-S.; Islam, M. A.; Kang, S.-K.; Cho, M.-H.; Choi, Y.-J.; Cho, C.-S. *Biomaterials* **2012**, *33*, 7272–7281.

(15) Fichter, K. M.; Ingle, N. P.; McLendon, P. M.; Reineke, T. M. *ACS Nano* **2013**, *7*, 347–364.

(16) Attia, A. B. E.; Oh, P.; Yang, C.; Tan, J. P. K.; Rao, N.; Hedrick, J. L.; Yang, Y. Y.; Ge, R. *Small* **2014**, 21, 4281–4286.

(17) Engler, A. C.; Ke, X.; Gao, S.; Chan, J. M. W.; Coady, D. J.; Ono, R. J.; Lubbers, R.; Nelson, A.; Yang, Y. Y.; Hedrick, J. L. *Macromolecules* **2015**, 48, 1673–1678.

(18) Ge, L.; Qi, W.; Wang, L.; Miao, H.; Qu, Y.; Li, B.; Song, B. *Proc. Natl. Acad. Sci. U. S. A.* **2011**, *108*, 551–556.

(19) Chu, B.; Liao, Y.; Qi, W.; Xie, C.; Du, X.; Wang, J.; Yang, H.; Miao, H.; Li, B.; Song, B. *Cell* **2015**, *161*, 291–306.

(20) Tabas, I. *J. Clin. Invest.* **2002**, *110*, 905–911.

(21) Chytil, P.; Etrych, T.; Konák, C.; Sírová, M.; Mrkvan, T.; Boucek, J.; Říhová, B.; Ulbrich, K. *J. Control. Release* **2008**, *127*, 121–130.

(22) Lee, A. L. Z.; Venkataraman, S.; Sirat, S. B. M.; Gao, S.; Hedrick, J. L.; Yang, Y. Y. *Biomaterials* **2012**, *33*, 1921–1928.

(23) Sevimli, S.; Sagnella, S.; Macmillan, A.; Whan, R.; Kavallaris, M.; Bulmus, V.; Davis, T. P. *Biomater. Sci.* **2015**, *3*, 323–335.

(24) He, Z.; Chu, B.; Wei, X.; Li, J.; Edwards, C. K.; Song, X.; He, G.; Xie, Y.; Wei, Y.; Qian, Z. *Int. J. Pharm.* **2014**, *469*, 168–178.

(25) Hosta-Rigau, L.; Zhang, Y.; Teo, B. M.; Postma, A.; Städler, B. *Nanoscale* **2013**, *5*, 89–109.

(26) Zhou, Y.; Briand, V. A.; Sharma, N.; Ahn, S.; Kasi, R. M. *Materials* **2009**, *2*, 636–660.

(27) Ercole, F.; Whittaker, M. R.; Quinn, J. F.; Davis, T. P. *Biomacromolecules* **2015**, 16, 1886-1914.

(28) Hu, F.; Chen, S.; Li, H.; Sun, J.; Sheng, R.; Luo, T.; Cao, A. *Acta Chim. Sin.* **2013**, *71*, 351-359.

(29) Chen, S.; Hu, F.; Sheng, R.; Cao, A. *Acta Polym. Sin.* **2013**, *13*, 102–111.

(30) Jia, L.; Liu, M.; Di Cicco, A.; Albouy, P.-A.; Brissault, B.; Penelle, J.; Boileau, S.; Barbier, V.; Li, M.-H. *Langmuir* **2012**, *28*, 11215–11224.

(31) Jia, L.; Albouy, P.-A.; Di Cicco, A.; Cao, A.; Li, M.-H. *Polymer* **2011**, *52*, 2565–2575.

(32) Jia, L.; Lévy, D.; Durand, D.; Impéror-Clerc, M.; Cao, A.; Li, M.-H. *Soft Matter* **2011**, *7*, 7395-7403.

(33) Jia, L.; Cao, A.; Lévy, D.; Xu, B.; Albouy, P.-A.; Xing, X.; Bowick, M. J.; Li, M.-H. *Soft Matter* **2009**, *5*, 3446-3451.

(34) Tran, T.; Nguyen, C. T.; Gonzalez-Fajardo, L.; Hargrove, D.; Song, D.; Deshmukh, P.; Mahajan, L.; Ndaya, D.; Lai, L.; Kasi, R. M.; Lu, X. *Biomacromolecules* **2014**, *15*, 4363–4375.

(35) Jia, L.; Cui, D.; Bignon, J.; Di Cicco, A.; Wdzieczak-Bakala, J.; Liu, J.; Li, M.-H. *Biomacromolecules* **2014**, *15*, 2206–2217.

(36) Mura, S.; Nicolas, J.; Couvreur, P. *Nat. Mater.* **2013**, *12*, 991–1003.

(37) Ganta, S.; Devalapally, H.; Shahiwala, A.; Amiji, M. *J. Control. Release* **2008**, *126*, 187–204.

(38) Wei, H.; Zhuo, R.; Zhang, X. *Prog. Polym. Sci.* **2013**, *38*, 508–535.

(39) Dai, S.; Ravi, P.; Tam, K. C. *Soft Matter* **2008**, *4*, 435-449.

(40) Lou, S.; Gao, S.; Wang, W.; Zhang, M.; Zhang, J.; Wang, C.; Li, C.; Kong, D.; Zhao, Q. *Nanoscale* **2015**, *7*, 3137–3146.

(41) Pan, Y.; Chen, Y.; Wang, D.; Wei, C.; Guo, J.; Lu, D.; Chu, C.; Wang, C. *Biomaterials* **2012**, *33*, 6570–6579.

(42) Shalviri, A.; Chan, H. K.; Raval, G.; Abdekhodaie, M. J.; Liu, Q.; Heerklotz, H.; Wu, X. *Colloids Surf. B. Biointerfaces* **2013**, *101*, 405–413.

(43) Moad, G.; Chong, Y. K.; Postma, A.; Rizzardo, E.; Thang, S. H. *Polymer.* **2005**, *46*, 8458–8468.

(44) Wei, Z.; Hao, X.; Gan, Z.; Hughes, T. C. *J. Polym. Sci. Part A Polym. Chem.* **2012**, *50*, 2378–2388.

(45) Lv, S.; Li, M.; Tang, Z.; Song, W.; Sun, H.; Liu, H.; Chen, X. *Acta Biomater.* **2013**, *9*, 9330–9342.

(46) Ghadban, A.; Albertin, L. *Polymers* **2013**, *5*, 431–526.

(47) Lowe, A. B.; Wang, R. *Polymer* **2007**, *48*, 2221–2230.

(48) Sevimli, S.; Inci, F.; Zareie, H. M.; Bulmus, V. *Biomacromolecules* **2012**, *13*, 3064–3075.

(49) Jiang, X.; Zhao, B. *Macromolecules* **2008**, *41*, 9366–9375.

(50) Pin, Rafaelol, Jia, L.; Gubellini, F.; Le, D.; Albouy, P.; Keller, P. *Macromolecules* **2007**, *40*, 16–18.

(51) Khong, Y. K.; Gan, S. N. *J. Appl. Polym. Sci.* **2013**, *130*, 153–160.

(52) Kulthe, S. S.; Choudhari, Y. M.; Inamdar, N. N.; Mourya, V. *Des. Monomers Polym.* **2012**, *15*, 465–521.

(53) Kataoka, K.; Harada, A.; Nagasaki, Y. *Adv. Drug Deliv. Rev.* **2001**, *47*, 113–131.

(54) Kamimura, M.; Kim, J. O.; Kabanov, A. V; Bronich, T. K.; Nagasaki, Y. *J. Control. Release* **2012**, *160*, 486–494.

(55) Guan, X.; Li, Y.; Jiao, Z.; Chen, J.; Guo, Z.; Tian, H.; Chen, X. *Acta Biomaterialia* **2013**, *9*, 7672–7678.

(56) Yan, J.; Ye, Z.; Chen, M.; Liu, Z.; Xiao, Y.; Zhang, Y.; Zhou, Y.; Tan, W.; Lang, M. *Biomacromolecules* **2011**, *12*, 2562–2572.

(57) Chang, L.; Deng, L.; Wang, W.; Lv, Z.; Hu, F.; Dong, A.; Zhang, J. *Biomacromolecules* **2012**, *13*, 3301–3310.

(58) Liu, Y.; Wang, Y.; Zhuang, D.; Yang, J.; Yang, J. *J. Colloid Interface Sci.* **2012**, *377*, 197–206.

(59) Lee, A. L. Z.; Venkataraman, S.; Sirat, S. B. M.; Gao, S.; Hedrick, J. L.; Yang, Y. Y. *Biomaterials* **2012**, *33*, 1921–1928.

(60) Du, Y.; Chen, W.; Zheng, M.; Meng, F.; Zhong, Z. *Biomaterials* **2012**, *33*, 7291–7299.

(61) Yang, Y.; Pan, D.; Luo, K.; Li, L.; Gu, Z. *Biomaterials* **2013**, *34*, 8430–8443.

(62) Hao, Y.; He, J.; Li, S.; Liu, J.; Zhang, M.; Ni, P. *J. Mater. Chem. B* **2014**, *2*, 4237–4249.

(63) Satoh, M. S.; Lindahl, T. *Nature* **1992**, *356*, 356–358.

(64) Nicholson, D. W.; Ali, A.; Thornberry, N. A.; Vaillancourt, J. P.; Ding, C. K.; Gallant, M.; Gareau, Y.; Griffin, P. R.; Labelle, M.; Lazebnik, Y. A. *Nature* **1995**, *376*, 37–43.

(65) Oliver, F. J. *J. Biol. Chem.* **1998**, *273*, 33533–33539.

Table of Content (TOC)

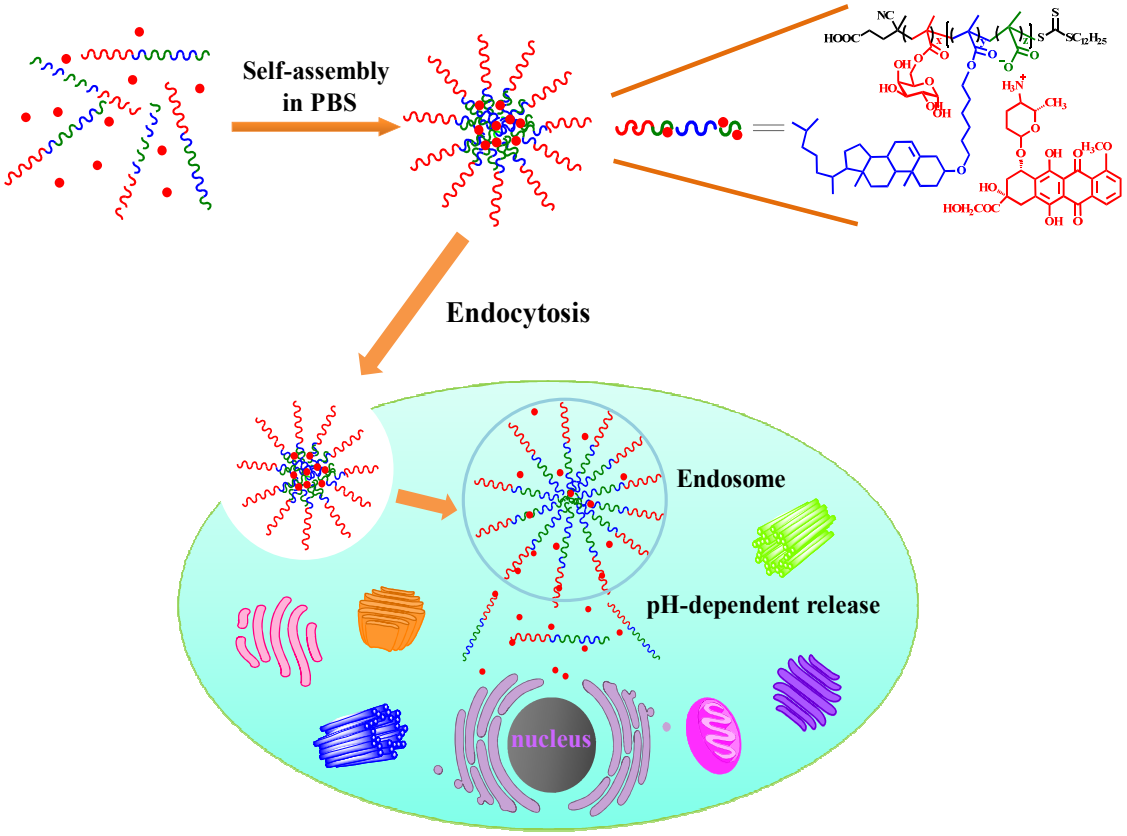

Scheme 1 Synthetic Pathways for the Comonomers of MAIpGP (A), MAChol (B) and Amphiphilic Diblock Terpolymer PMAgala-*b*-P(MAA-*co*-MAChol)s (C)

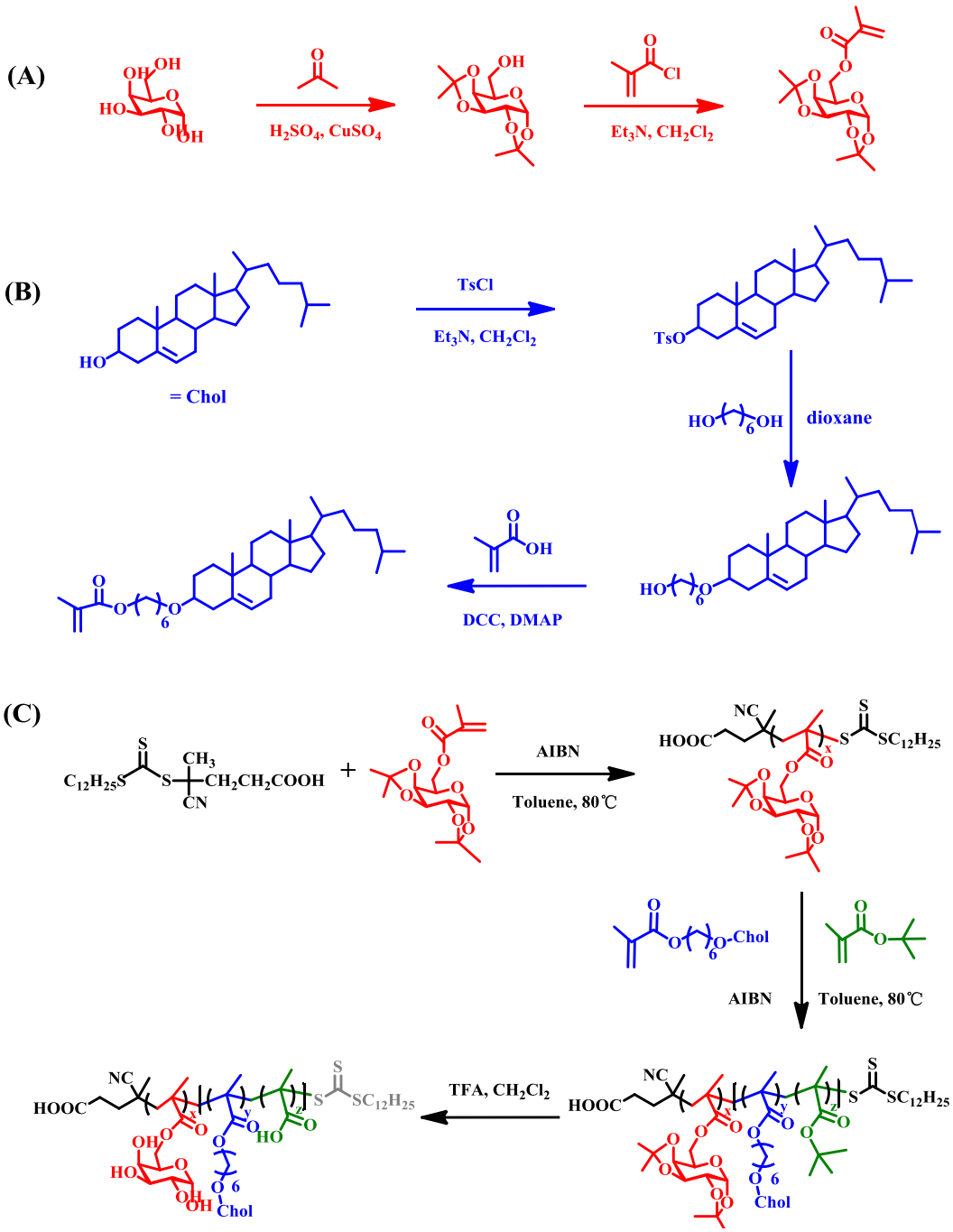

Scheme 2 Efficient Loading and Intracellular Release of The Doxorubicin (DOX) by pH-Responsive Micelles of New Amphiphilic Diblock Terpolymer PMAgala-*b*-P(MAA-*co*-MAChol)s Bearing Pendant Galactose and Cholesterol

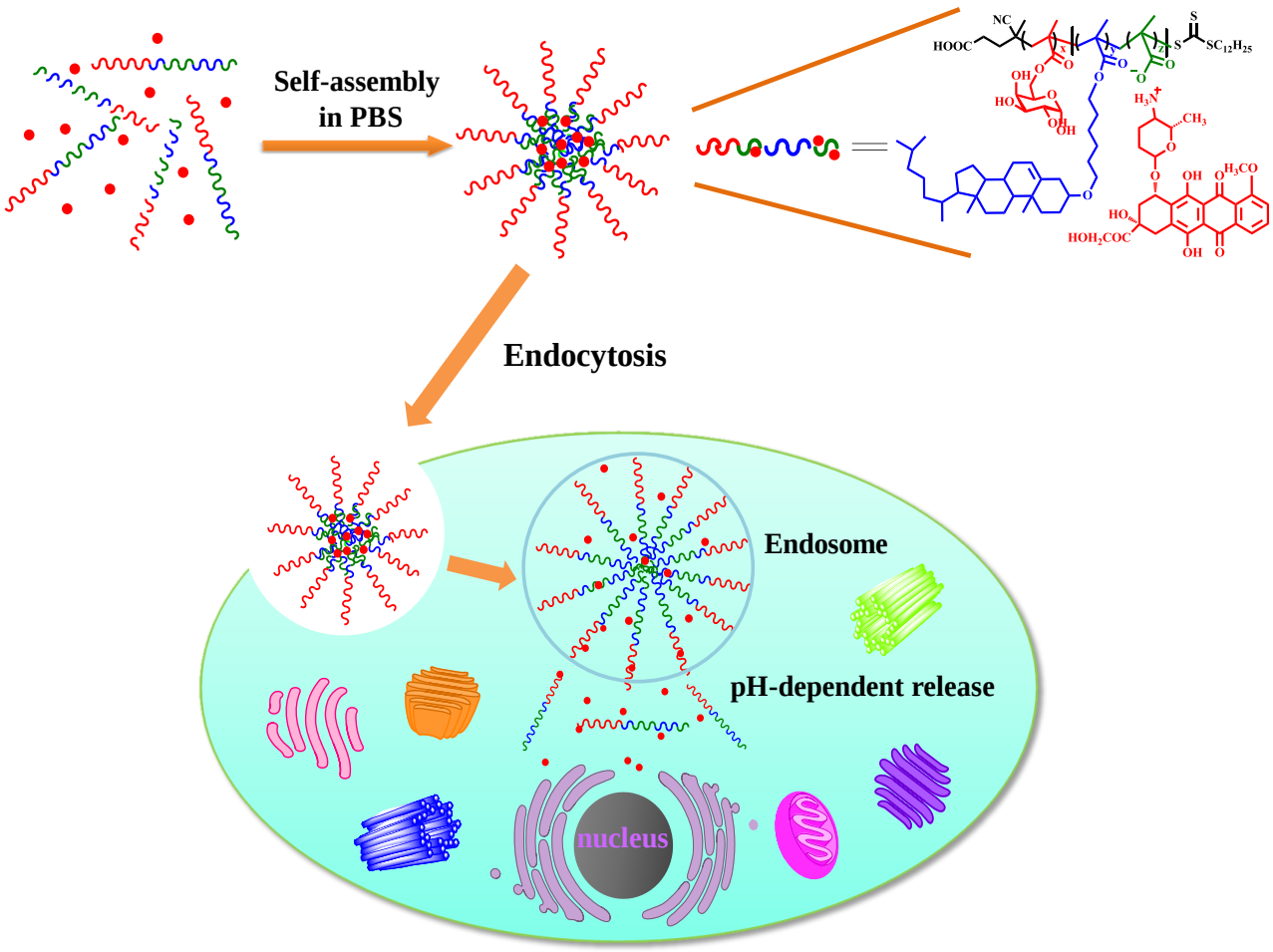

Table 1 Characteristics of the Synthesized Macro-RAFT Initiator PMAIpGP and Diblock Terpolymer PMAIpGP-*b*-P(*t*BMA-*co*-MAChol)s

Entry [a]	Sample	Conv. (%) [b]	$M_{n,conv}$ [e] (kg/mol)	$M_{n,GPC}$ [f] (kg/mol)	$M_{w,GPC}$ [f] (kg/mol)	M_w/M_n [f]	x [g]	y [g]	z [g]	m/n/p [h]
1	$PMAIpGP_{18}$	90	6.32	4.92	5.56	1.12	18	-	-	
2	$PMAIpGP_{18}$-*b*-$PMAChol_{14}$	85	13.9	12.8	16.2	1.26	18	-	14	36/-/64
3	$PMAIpGP_{18}$-*b*-P(^{t}BMA_5-*co*-$MAChol_{14}$)	100[c],70[d]	14.8	13.1	15.3	1.17	18	5	14	34/3/63
4	$PMAIpGP_{18}$-*b*-P(^{t}BMA_{16}-*co*-$MAChol_{12}$)	100[c], 90[d]	15.3	16.6	18.8	1.13	18	16	12	35/11/54
5	$PMAIpGP_{18}$-*b*-P(^{t}BMA_{26}-*co*-$MAChol_9$)	88[c], 90[d]	15.0	16.2	19.5	1.20	18	26	9	37/19/44

Notes: [a] The initial CDP/MAIpGP/AIBN feeding molar ratio of entry 1 was 1/20/0.2, and initial macro-RAFT/ ^{t}BMA/MAChol/AIBN feeding molar ratio of entry 2 to entry 5 were 1/0/16/0.2, 1/5/20/0.2, 1/16/13/0.2 and 1/30/10/0.2, respectively. [b]Monomer conversion was determined by ^{1}H NMR. [c, d]Data express the monomer conversions of ^{t}BMA and MAChol, respectively. [e]The $M_{n,conv}$ values were calculated by the monomer conversions. [f] Data mean number-average molar mass (M_n), weight-average molar mass (M_w) and polydispersity index (M_w/M_n) determined by GPC with polystyrene (PS) standards. [g]x, y and z represent average degrees of polymerization (DP) for the MAIpGP, ^{t}BMA and MAChol comonomer, respectively, and were evaluated by the comonomer conversions. [h] m, n, p represent weight percentages of MAgala, MAA and MAChol respectively

.

Table 2 Particle Sizes and Zeta Potentials as well as the DOX-Loading Efficiencies for the Amphiphilic Diblock Terpolymer Micelles

Sample	Blank micelles				DOX-loaded micelles				
	Size (nm)[a]	PDI[a]	Zeta (mv)[a]	CMC[b] (mg/L)	Size (nm)[a]	PDI[a]	Zeta (mv)[a]	DLC (wt%)[c]	DLE (%)[c]
PMAgala$_{18}$-*b*-PMAChol$_{14}$	140.2±1.2	0.156	-14.8±2.6	2.82	243.9±5.6	0.214	-12.2±0.8	10.5	47.1
PMAgala$_{18}$-*b*-P(MAA$_5$-*co*-MAChol$_{14}$)	48.9±0.5	0.104	-22.4±0.7	2.63	189.2±5.7	0.234	-19.6±0.9	13.3	61.5
PMAgala$_{18}$-*b*-P(MAA$_{16}$-*co*-MAChol$_{12}$)	68.1±1.1	0.228	-28.0±0.6	1.41	117.8±1.8	0.179	-26.9±0.4	17.0	81.9
PMAgala$_{18}$-*b*-P(MAA$_{26}$-*co*-MAChol$_9$)	94.9±1.1	0.227	-31.4±1.1	1.58	95.8±2.2	0.205	-26.4±2.0	18.6	91.2

Notes: [a] Data express the average sizes, polydispersity indices (PDI) and zeta potentials of amphiphilic copolymer micelles formed in PBS buffer (pH 7.4, 10 mM) by DLS at 25 ^{o}C. [b]Values indicate the critical micelle concentration (CMC) determined by a fluorescence spectrometer using a pyrene probe. [c] The data were calculated with a theoretical DOX loading content of 20 wt%.

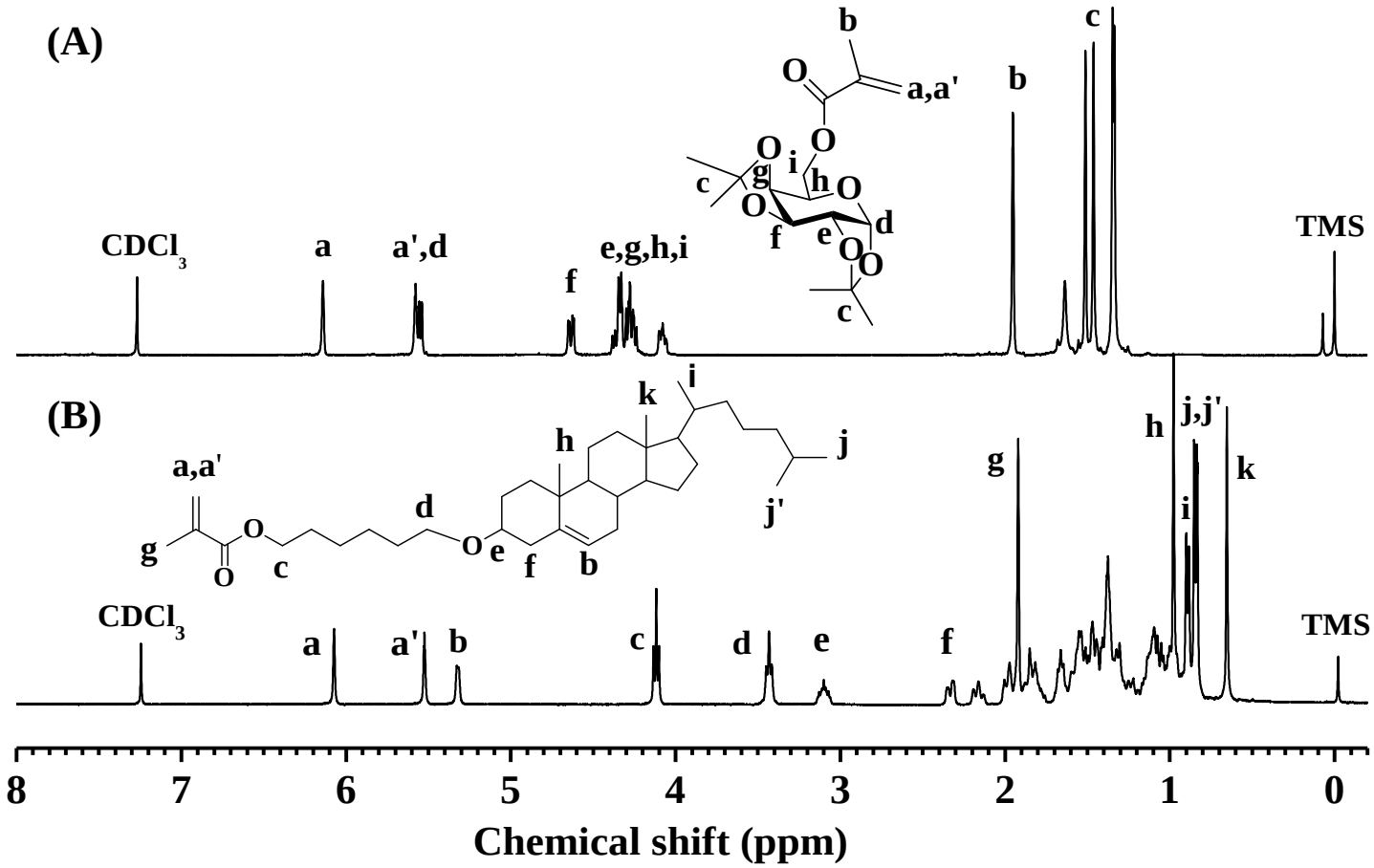

Figure 1 ^{1}H NMR spectra of the synthesized monomers of MAIpGP (A) and MAChol (B) in $CDCl_3$

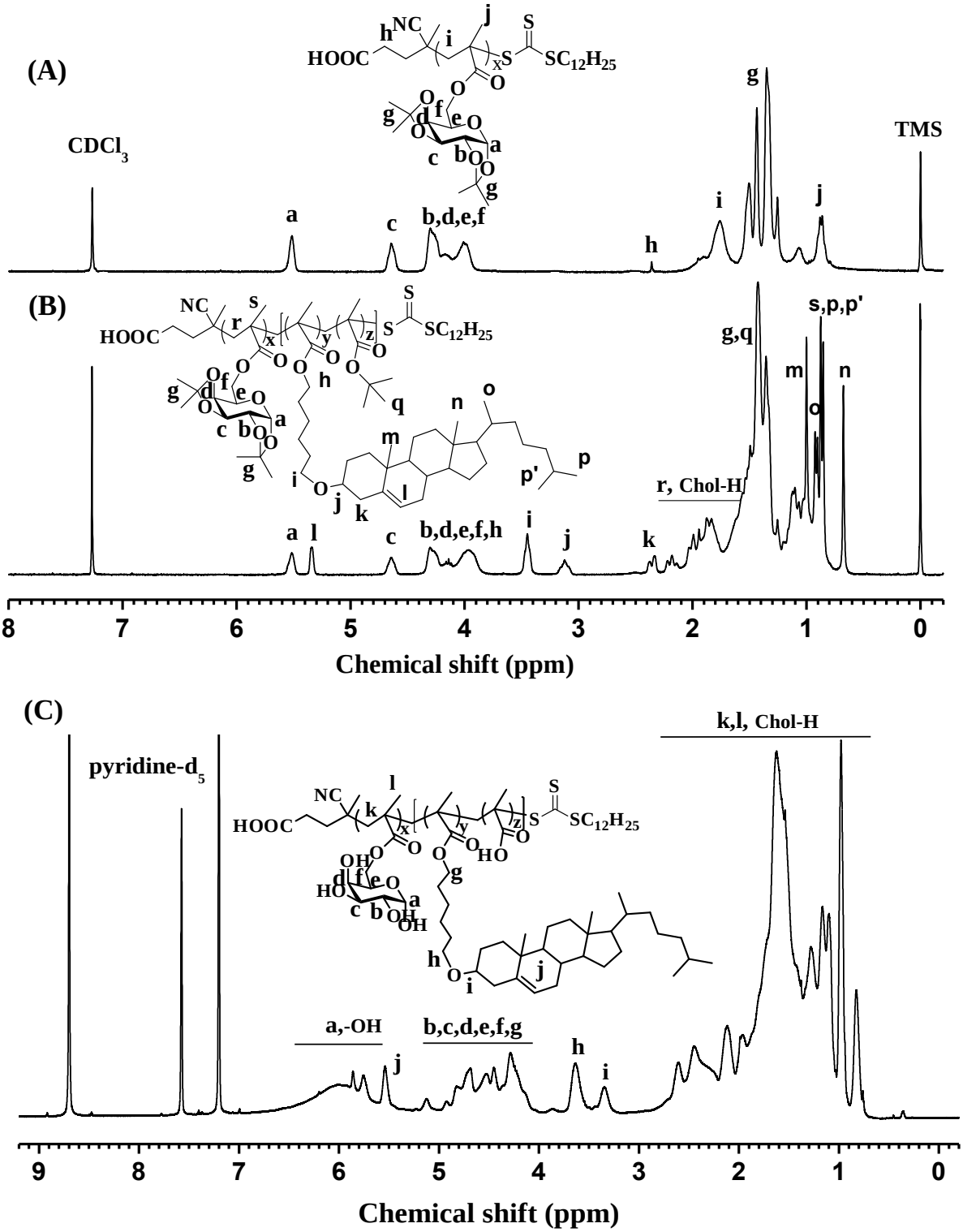

Figure 2 ^{1}H NMR spectra of the macro-RAFT initiator $PMAIpGP_{18}$ (A), diblock terpolymer $PMAIpGP_{18}$-*b*-P($^{t}BMA_{16}$-*co*-$MAChol_{12}$) (B) in $CDCl_3$ at room temperature as well as $PMAgala_{18}$-*b*-P(MAA_{16}-*co*-$MAChol_{12}$) amphiphiles (C) in pyridine-d_5 at 80 ^{o}C

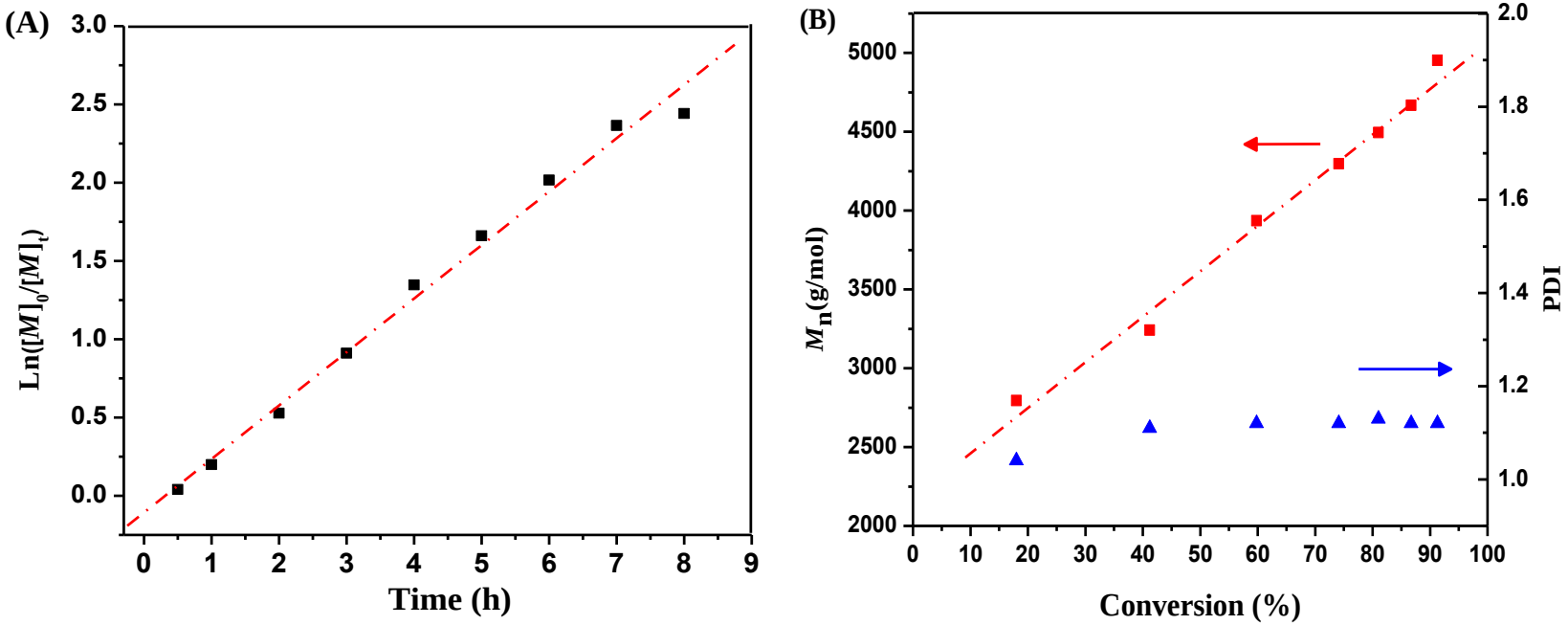

Figure 3 Kinetics of RAFT polymerization of the MAIpGP monomer at 80°C in toluene. (A) kinetic plot of the Ln($[M]_0/[M]_t$) as a function of reaction time, (B) monomer conversion dependence of number average molecular weights (M_n) (■) and PDI(▲) of the products

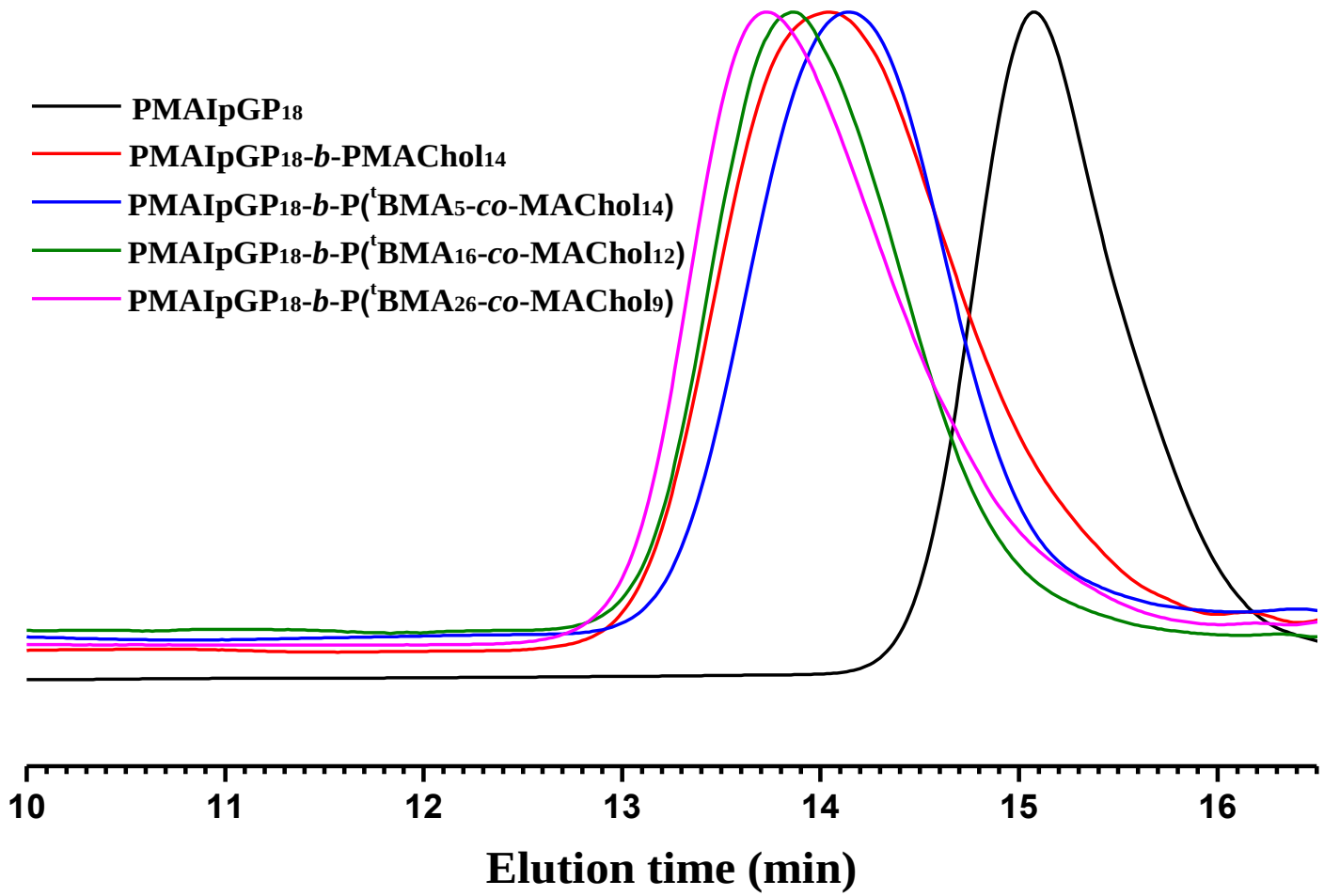

Figure 4 GPC elution traces of the diblock terpolymer PMAIpGP-*b*-P(^{t}BMA-*co*-MAChol)s along with their macro-RAFT initiator PMAIpGP$_{18}$

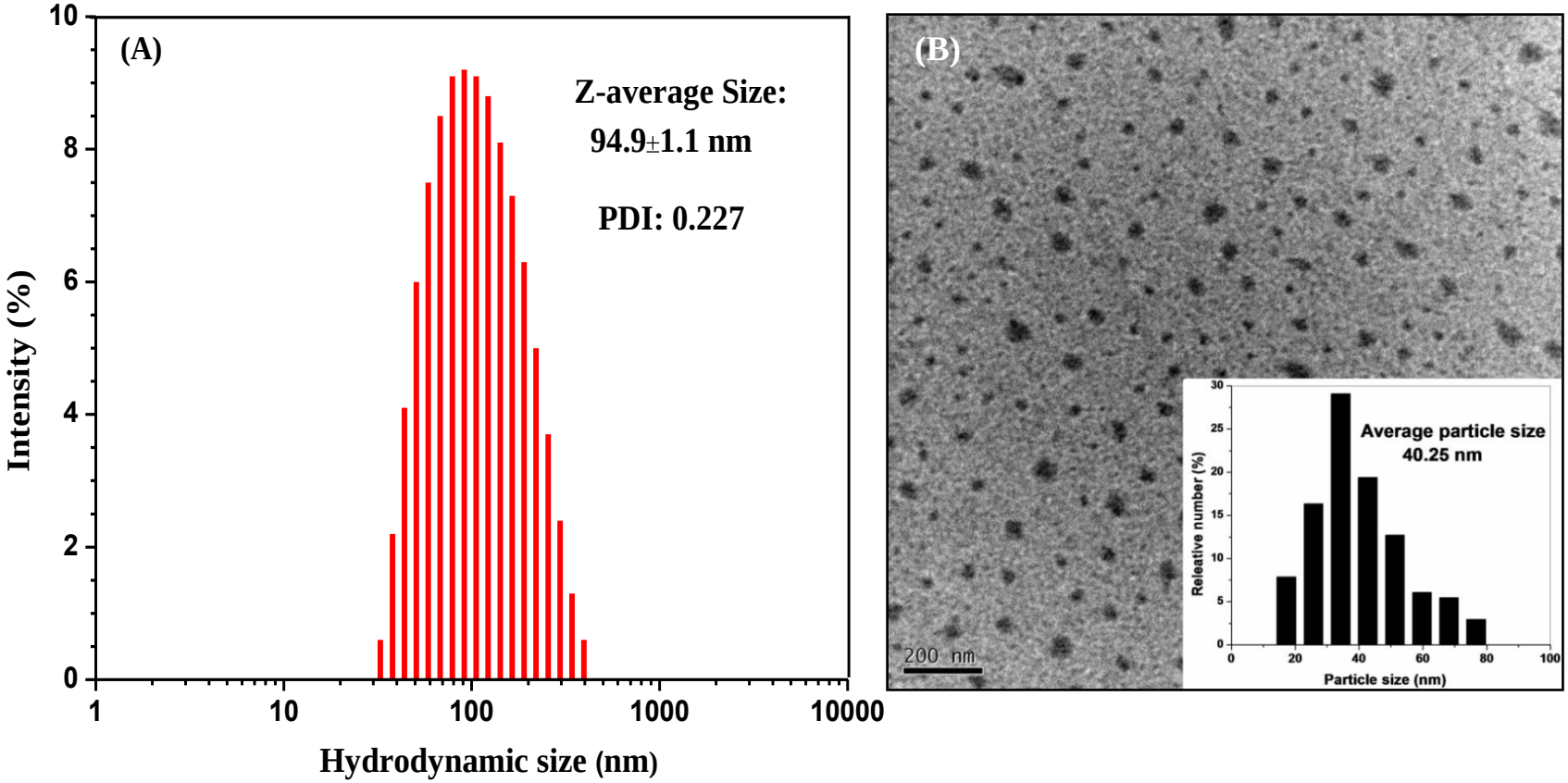

Figure 5 Sizes and morphologies of the amphiphilic diblock terpolymer PMAgala$_{18}$-*b*-P(MAA$_{26}$-*co*-MAChol$_9$) micelles measured by dynamic light scattering (DLS) (A) and TEM (B), respectively

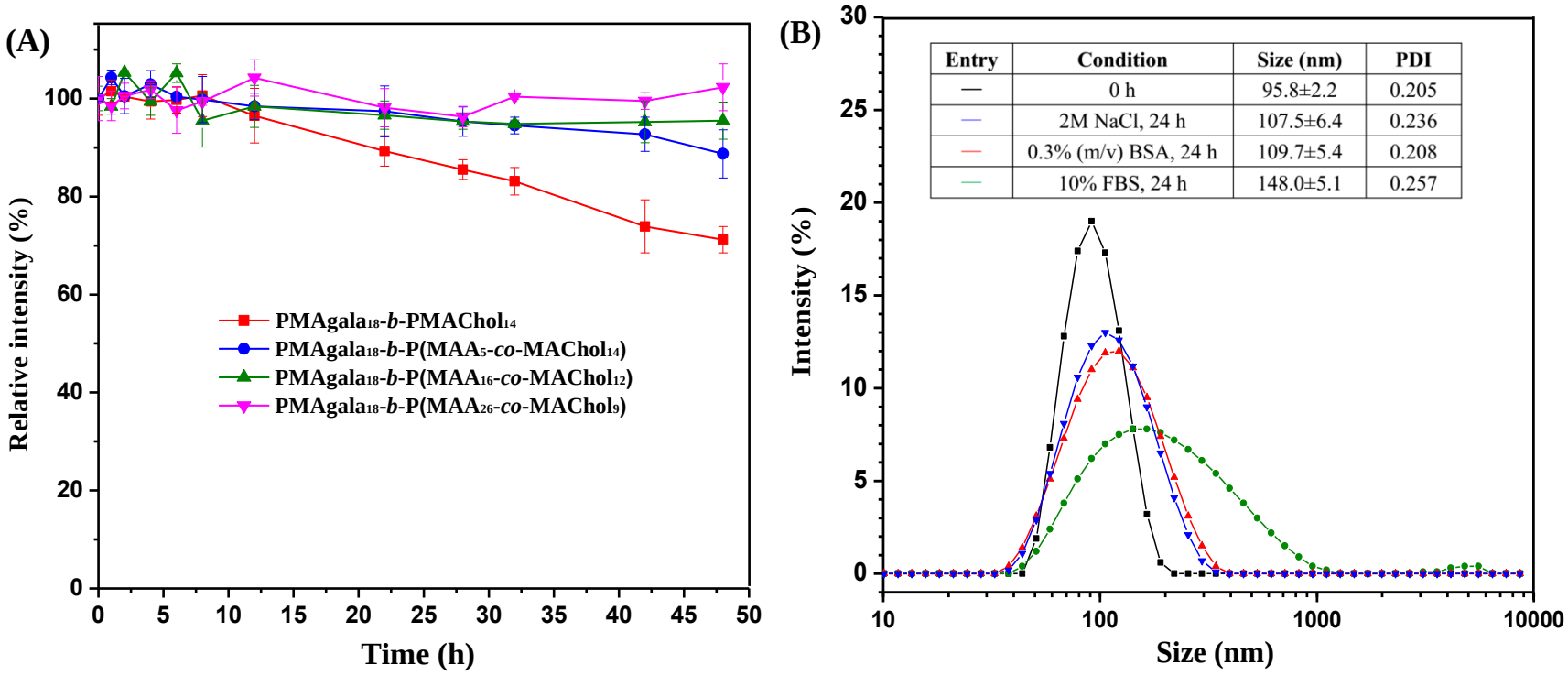

Figure 6 Particle stability of the DOX-loaded amphiphilic diblock terpolymer micelles (1.0 mg/mL) at 37°C in aqueous solution assayed by DLS. (A) Profile of the time dependence of relative scattered laser light intensities upon adding SDS surfactant (100 μg/mL); (B) Sizes of the PMAgala$_{18}$-*b*-P(MAA$_{26}$-*co*-MAChol$_9$)/DOX micelles in the presence of NaCl, BSA or FBS

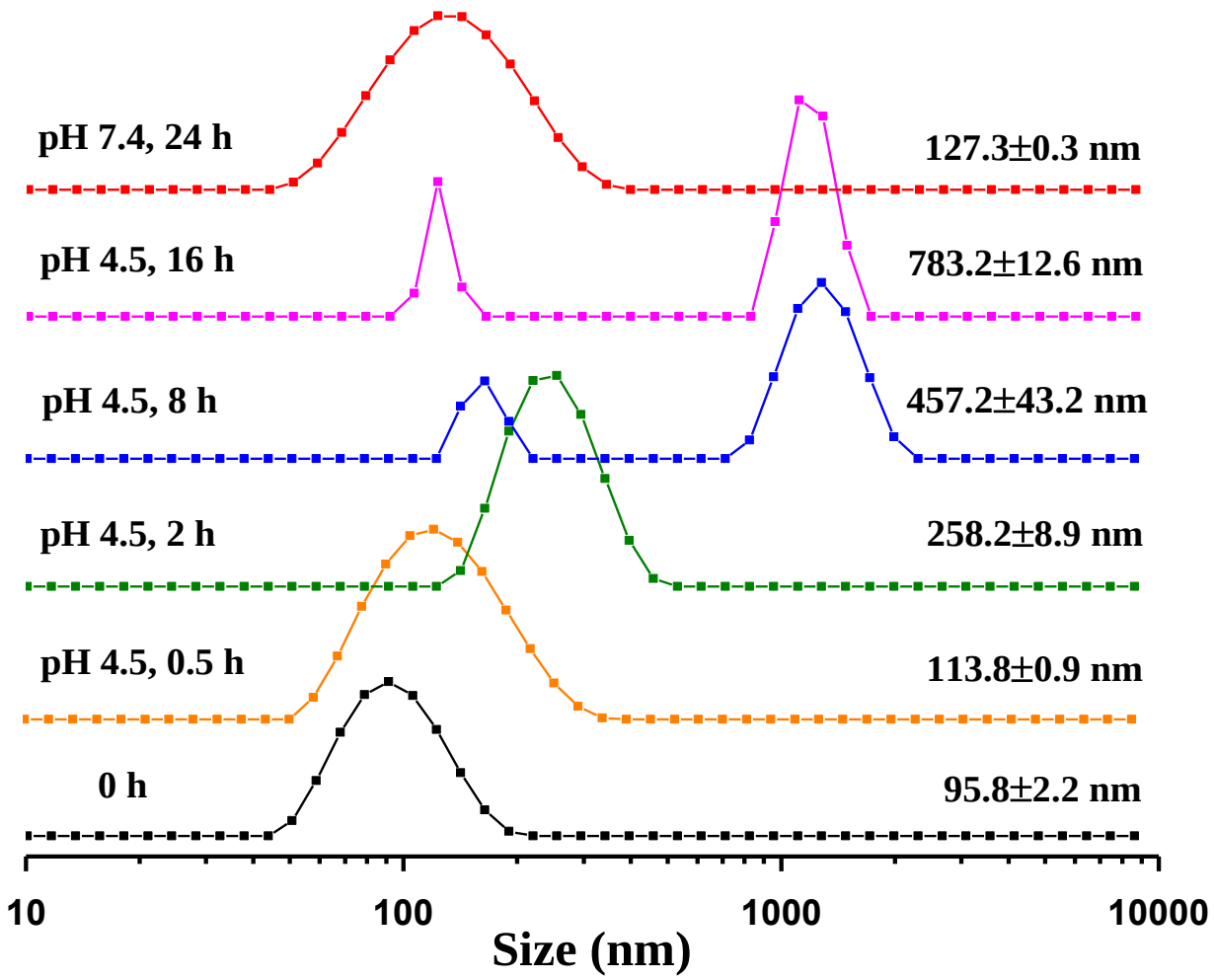

Figure 7 pH responsive particle sizes of the DOX-loaded PMAgala$_{18}$-*b*-P(MAA$_{26}$-*co*-MAChol$_9$) micelles at 37 ^{o}C in acetate buffer (pH 4.5,10 mM) or phosphate buffer (pH 7.4, 10 mM) by DLS

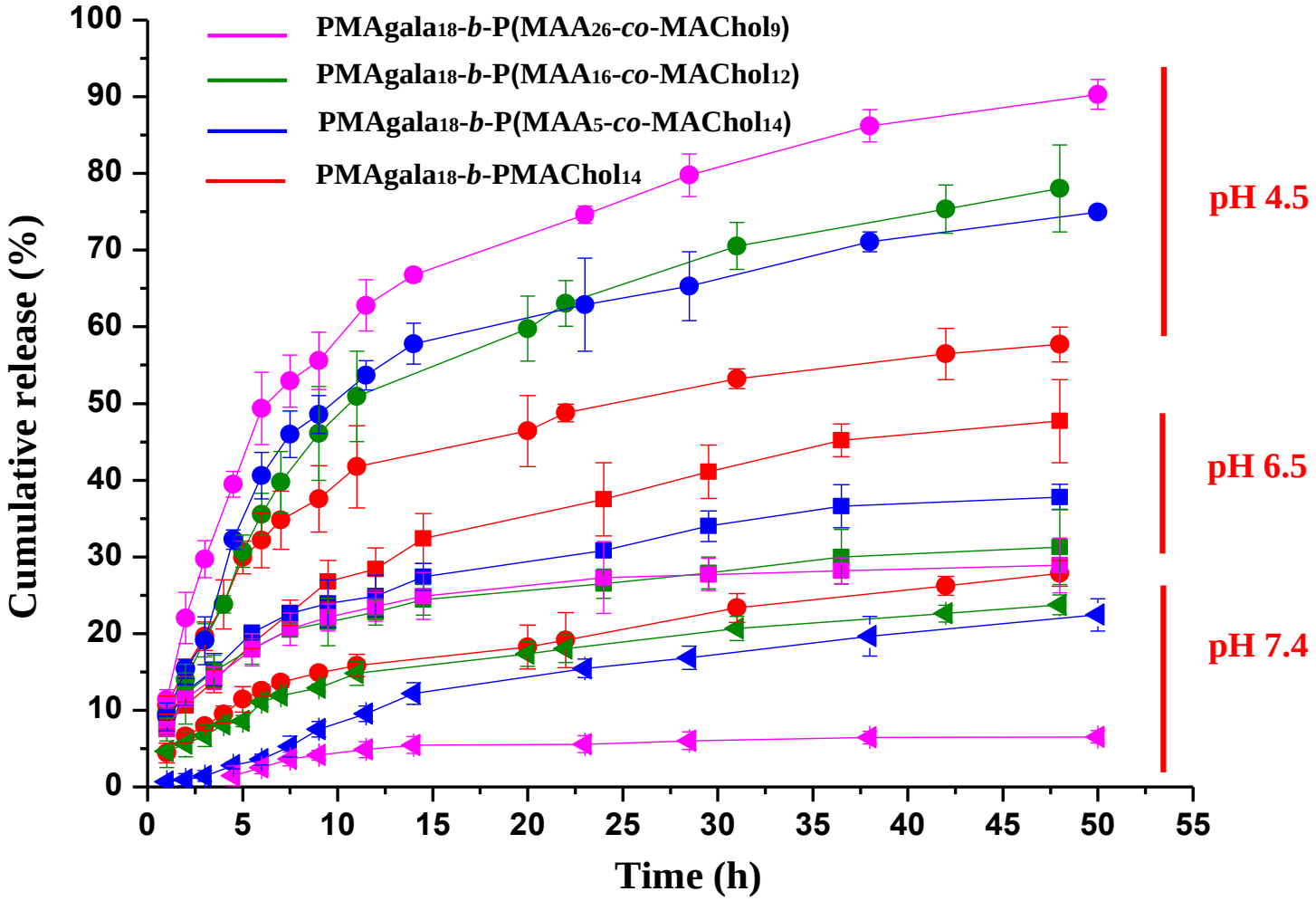

Figure 8 *In vitro* drug release profiles of the DOX-loaded amphiphilic diblock terpolymer micelles at 37 ℃ under different pH conditions: phosphate buffer (pH 7.4, 10 mM), phosphate buffer (pH 6.5, 10 mM) and acetate buffer (pH 4.5, 10 mM), respectively

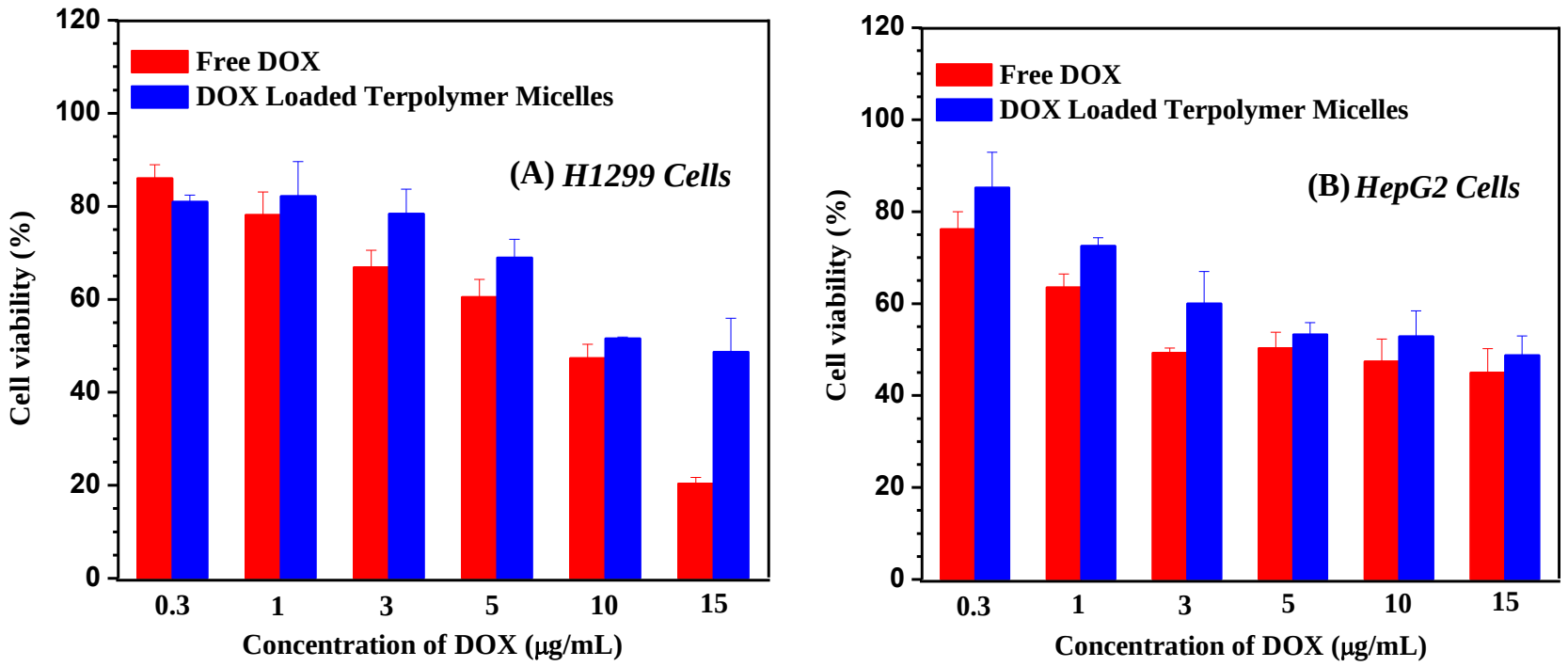

Figure 9 Cell viability assay of the DOX-loaded PMAgala$_{18}$-*b*-P(MAA$_{26}$-*co*-MAChol$_9$) micelles and free DOX under different DOX dosages after 30 h incubation with H1299 cells (A) and HepG2 cells (B)

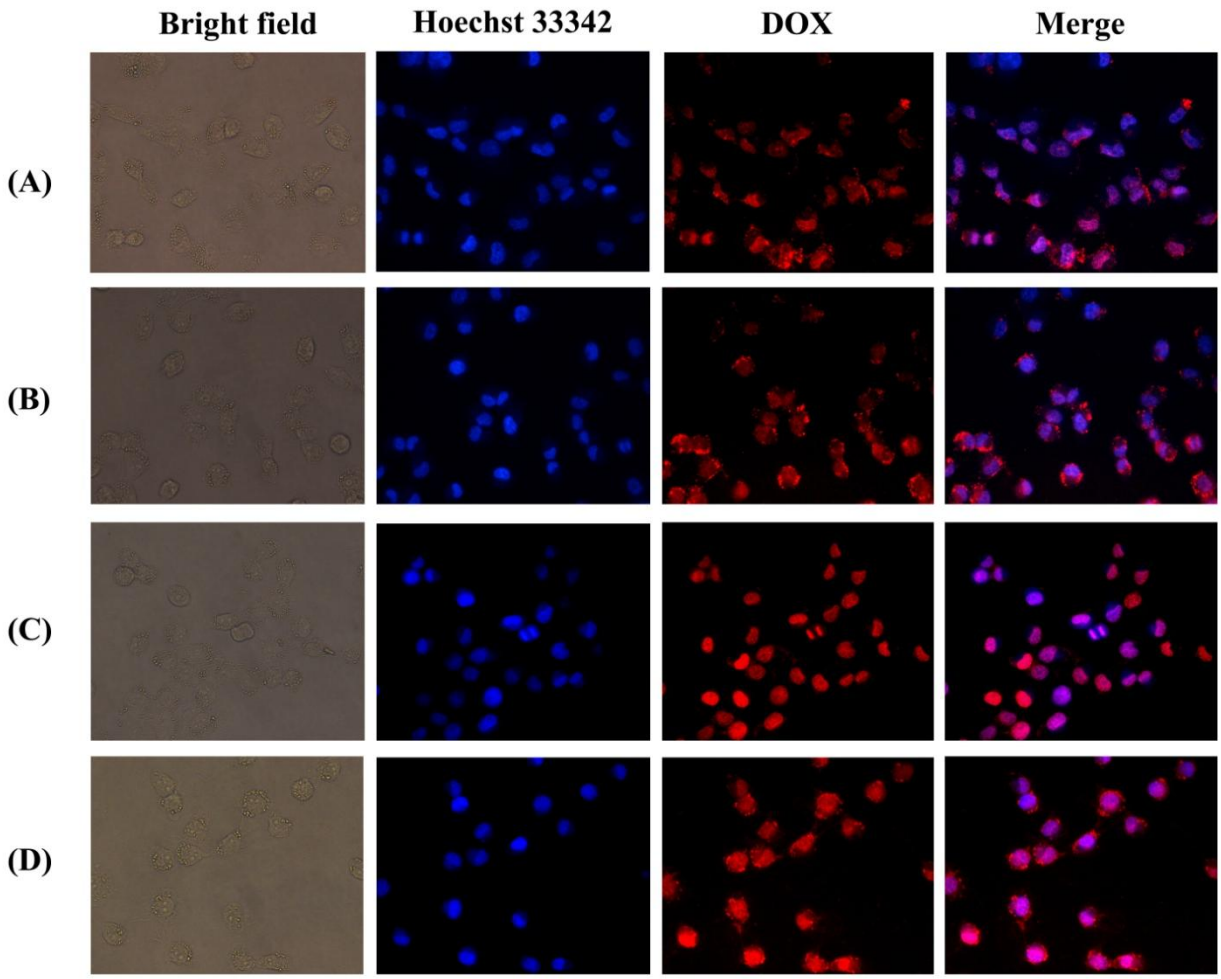

Figure 10 Fluorescence images (400×) of the H1299 cells after free DOX treatment for 1 h (A) and 6 h (C), and with DOX-loaded PMAgala$_{18}$-*b*-P(MAA$_{26}$-*co*-MAChol$_9$) micelles for 1 h (B) and 6 h (D). The DOX dosage was fixed to be 10 μg/mL, and the pictures from left to right indicate the results of bright field, nuclei-stained cells by Hoechst 33342 (blue), fluorescence image of the DOX (red) as well as their overlays

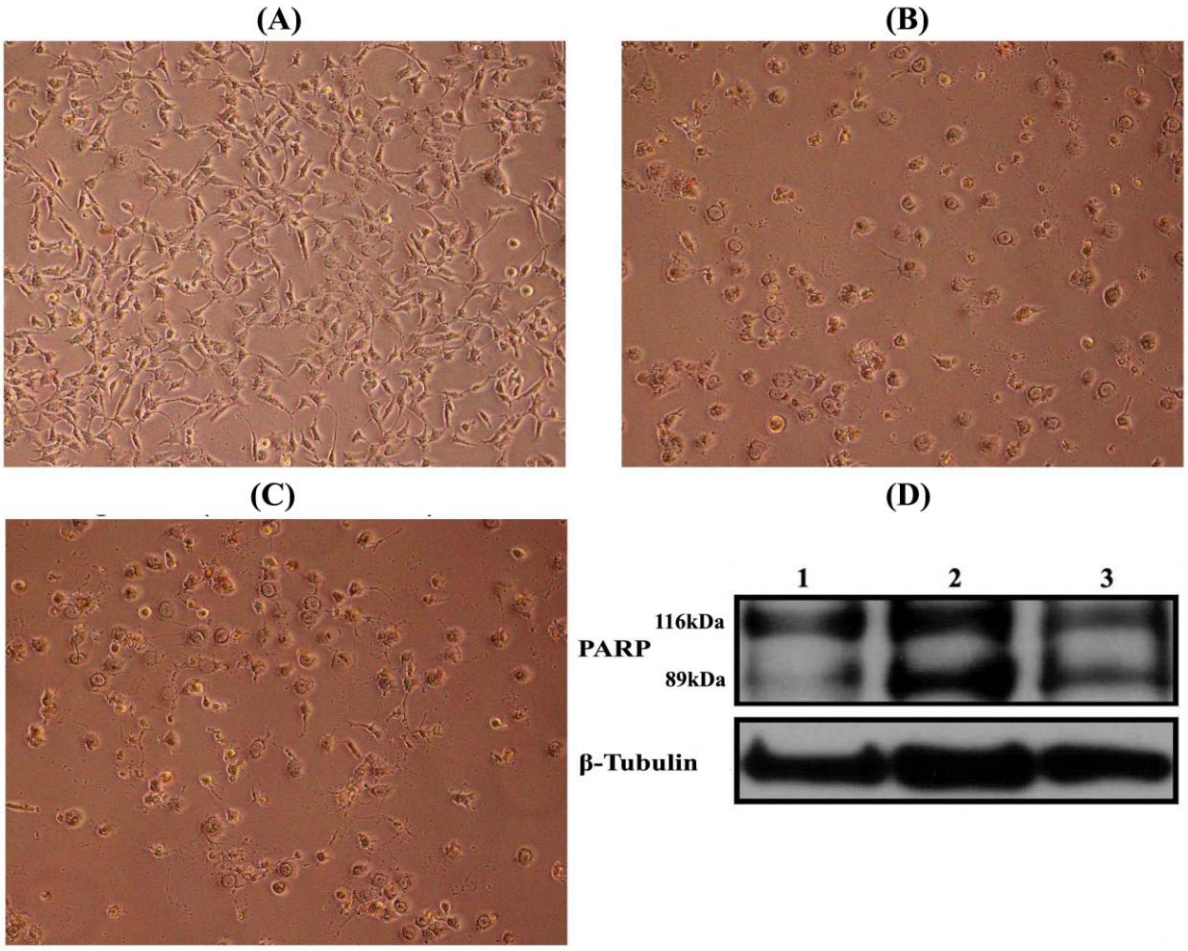

Figure 11 Morphologies of the H1299 cells and the results of western blot detection after the treatment with either free DOX or DOX-loaded terpolymer micelles under a DOX dosage of 10 μg/mL for 30 h. (A) blank control (cell culture plate); (B) free DOX; (C) DOX-loaded PMAgala$_{18}$-*b*-P(MAA$_{26}$-*co*-MAChol$_9$) micelles; (D) Cleavage of the PARP tested by western blot where the line 1 to line 3 represent the results of blank control, free DOX and DOX-loaded micelles, respectively